


# A genome-wide association study identifies novel players in Na and Fe homeostasis in *Arabidopsis thaliana* under alkaline-salinity stress

Maria Jose Almira Casellas<sup>1,†</sup> , Laura Pérez-Martín<sup>1,2,†</sup> , Silvia Busoms<sup>1</sup> , René Boesten<sup>3</sup> , Mercè Llugany<sup>1</sup> , Mark G. M. Aarts<sup>3,\*</sup>  and Charlotte Poschenrieder<sup>1,\*</sup> 

<sup>1</sup>Plant Physiology Laboratory, Bioscience Faculty, Universitat Autònoma de Barcelona, C/de la Vall Moronta s/n, E-08193, Bellaterra, Spain,

<sup>2</sup>Department of Botany and Plant Biology, University of Geneva, 1211, Geneva, Switzerland, and

<sup>3</sup>Laboratory of Genetics, Wageningen University and Research, Droevendaalsesteeg 1, 6708 PB, Wageningen, The Netherlands

Received 26 October 2022; revised 11 November 2022; accepted 21 November 2022; published online 17 December 2022.

\*For correspondence (e-mail charlotte.poschenrieder@uab.es and mark.aarts@wur.nl)

<sup>†</sup>These authors contributed equally.

## SUMMARY

In nature, multiple stress factors occur simultaneously. The screening of natural diversity panels and subsequent Genome-Wide Association Studies (GWAS) is a powerful approach to identify genetic components of various stress responses. Here, the nutritional status variation of a set of 270 natural accessions of *Arabidopsis thaliana* grown on a natural saline-carbonated soil is evaluated. We report significant natural variation on leaf Na (LNa) and Fe (LFe) concentrations in the studied accessions. Allelic variation in the *NINJA* and *YUC8* genes is associated with LNa diversity, and variation in the *ALA3* is associated with LFe diversity. The allelic variation detected in these three genes leads to changes in their mRNA expression and correlates with plant differential growth performance when plants are exposed to alkaline salinity treatment under hydroponic conditions. We propose that *YUC8* and *NINJA* expression patterns regulate auxin and jasmonic signaling pathways affecting plant tolerance to alkaline salinity. Finally, we describe an impairment in growth and leaf Fe acquisition associated with differences in root expression of *ALA3*, encoding a phospholipid translocase active in plasma membrane and the trans Golgi network which directly interacts with proteins essential for the trafficking of PIN auxin transporters, reinforcing the role of phytohormonal processes in regulating ion homeostasis under alkaline salinity.

**Keywords:** alkaline-salinity, GWAS, *Arabidopsis*, natural variation, ionome.

## INTRODUCTION

Plant responses to abiotic stress are presumably shaped by a combination of adaptation to the local environment, accumulation of mutations, gene flow between the populations and random effects. Local adaptation is particularly relevant in the face of the global changes our planet is exposed to, because locally adapted populations can become maladapted if environmental conditions change rapidly (Davila Olivas et al., 2017). When studying the genetic mechanisms and the extent of local adaptation, understanding the genetic basis of fitness variation across different ecological conditions is of major importance. This includes identifying the loci associated with individual fitness in different natural environments, the distribution

pattern and environment specificity of adaptive variants and the type of genes involved.

The diversity of stress responses present within one species can be harnessed by screening natural diversity panels and performing subsequent Genome-Wide Association Studies (GWAS) to identify genetic components of various stress responses, as has been done in the past for e.g., salinity (Baxter et al., 2010; Katori et al., 2010; Rus et al., 2006), carbonates (Pérez-Martín, 2020; Terés, 2017) or combinations of stress factors (Davila Olivas et al., 2017; Kawa et al., 2016). GWA studies enumerate underlying SNPs (single nucleotide polymorphisms) responsible for certain phenotypic traits by exploiting the natural variation in a population or collection of populations of the studied

species (Ogura & Busch, 2015; Weigel, 2012). More specifically, GWAS evaluate the statistical significance of associations between differences in a quantitative phenotype and genetic polymorphisms tested across many genetically different individuals by using linkage disequilibrium (LD), based on non-random association between alleles and phenotypes (Uffelmann et al., 2021). GWAS identifies associations between marker SNPs and phenotypes without the need of constructing special mapping populations, and it uses high recombination in natural populations instead (Bazakos et al., 2017; He et al., 2017; Korte & Farlow, 2013). The candidate genes identified by GWAS can eventually serve to guide marker-assisted breeding and the genetic modification of crops (Li, 2020). In this regard, recent reviews (Liu et al., 2020) point to GWA studies as an increasingly successful analysis in the identification of key genes that are useful for agronomic traits of interest.

In the model plant *Arabidopsis thaliana*, GWAS are a powerful approach to identify loci associated with fitness and abiotic stress responses. Multiple growth and reproductive life history traits showing natural variation along geographical gradients such as flowering time, seed dormancy, growth rate, resistance to abiotic stresses, defense related traits, ionome profile or root growth have proven to be good input data sets for GWA analyses. Atwell et al. (2010) demonstrated for the first time the power of GWAS for describing the genetics of natural variation in such traits in *A. thaliana*, many of them of great agricultural importance.

Stress resistance is one of the most ecologically relevant traits in a plant species. Due to its agronomic importance, salinity is among the most studied abiotic stress factors (Julkowska et al., 2014; Knight et al., 1997; Shabala et al., 2005). Since the start of GWAS in *A. thaliana*, important achievements have been obtained in revealing new genes and mapping new Quantitative Trait Loci (QTLs) for salinity tolerance. For example, by means of association mapping of ionome profile data of 394 *Arabidopsis* accessions, Baxter et al. (2010) identified *HKT1* as one of the major contributing factors to natural variation in  $\text{Na}^+$  accumulation in shoots. *HKT1* was previously known to be involved in sodium-driven potassium uptake (Rubio et al., 1995), sodium uniport in roots (Haro et al., 2005; Laurie et al., 2002), differential  $\text{Na}^+$  accumulation in aerial parts (Rus et al., 2006), and shoot  $\text{Na}^+$  exclusion and salt tolerance (Møller et al., 2009). *HKT1*, together with *CYTOCHROME P450 FAMILY 79 SUBFAMILY B2* and *B3* (*CYP79B2/B3*) were later confirmed as new components contributing to lateral root hair development under salt stress by performing GWAS on root traits from the *Arabidopsis* HapMap collection (Julkowska et al., 2017). GWA mapping of salinity tolerance in cultivars of interest like rice (Kumar et al., 2015; Nayeriprasad et al., 2021; Warraich et al., 2020), barley (Fan et al., 2016; Hazzouri

et al., 2018; Mwando et al., 2020), soybean (Do et al., 2019; Jin et al., 2021; Zeng et al., 2017; Zhang et al., 2019), cotton (Yasir et al., 2019), or wheat (Chaurasia et al., 2021) have been cutting-edge studies performed in recent years.

Alkaline-sodic environments are defined by a high  $\text{OH}^-$  concentration in the waters and soils accompanied by the dominance of sodium base cations in both dissolved and exchangeable forms. In this context, excess of dissolved carbonate species is required for the development of alkalinity and the increase of the dispersive power of sodium (Jobbágy et al., 2017). Soil carbonates have been much less explored through GWAS as a potential driving agent of natural variation. Most studies focus on the deficiency of iron (Mamidi et al., 2014; Satbhai et al., 2017, Assefa et al., 2020 and Xu et al., 2022, in *Arabidopsis*, chickpea, soybean and maize, respectively) or phosphorus (Liu et al., 2015 and Reddy et al., 2020, in mungbean) when studying the effects of alkalinity stress. The cited studies lead to the identification of new candidate iron responsive genes such as *AT1G01580/FRO2* (Mamidi et al., 2014; Satbhai et al., 2017) and *At5g53970/NAAT1*, *Os03g0237100/DMAS1*, *GRMZM5G812538/YSL11*, *AT4G19690/IRT1*, *AT1G10970/ZIP4* and *AT2G25490/EBF1* (Xu et al., 2022).

In nature, multiple stress factors occur simultaneously. Thus, assessing how plants respond to a combination of stresses is ecologically more representative of how their performance will be under field conditions. In areas with arid and semi-arid climates, like the Mediterranean region, soil salinity often co-occurs with alkalinity due to the movement of soluble ions like  $\text{Na}^+$ ,  $\text{Ca}^{2+}$ ,  $\text{Mg}^{2+}$ ,  $\text{K}^+$ ,  $\text{CO}_3^{2-}$  and  $\text{HCO}_3^-$  to the superficial soil layers produced by the increase in evapotranspiration rates (Singh, 2021). Alkaline-salinity stress has gained importance, in the last decade, as a major limiting factor for world crop production (Bai et al., 2018; Huang, 2018; Zhao et al., 2021). Around 831 million hectares of the Earth are covered by alkaline-saline soils (FAO, 1973). Alkaline-saline stress exerts complex harmful effects on plants in the form of osmotic pressure, ion toxicity, nutrient deficiency, and high pH (Liu et al., 2021). Alkaline salts inhibit germination, growth, photosynthesis, and root system activity, and are reported to increase shoot  $\text{Na}^+$  and ion imbalance with higher intensity than neutral salts in *Lathyrus quinquerivius* (Zhang & Mu, 2009). When compared to  $\text{NaCl}$  stress, alkaline-saline stress can increase the activities of  $\text{H}^+$ -ATPase and  $\text{H}^+$ -VPPases, which are proton-driven forces for  $\text{Na}$  transport at the cell and vacuolar membranes (Deinlein et al., 2014; Ye et al., 2019). Sodium sequestration into vacuoles takes place through *SOS2/SOS3* kinase-regulated *SOS1* and *NHX1*, a process sensitive to  $\text{Ca}^{2+}$  ions (Bahmani et al., 2015; Fang et al., 2021). Thus, adequate  $\text{Ca}$  levels are essential under alkaline salinity.

To a limited extent, alkaline salt tolerance has been explored by means of association mapping in the last decade. A major QTL allele from wild soybean was identified

for increasing alkaline salt tolerance (Tuyen et al., 2010). Epistatic association mapping in 257 soybean cultivars with 135 SSR markers was performed to assess salt tolerance under control, NaCl or Na<sub>2</sub>CO<sub>3</sub> conditions and small-effect QTLs were identified for further confirmation (Zhang et al., 2014). More recent association studies have provided novel candidate locus to crop breeders for improving saline-alkaline adaptation (Cao et al., 2020).

Here, we use a natural alkaline saline soil to assess the variation in growth and nutritional status in a set of 270 natural accessions of the widely distributed model species *A. thaliana* and we explore the molecular genetic mechanisms underlying possible stress responses to alkaline salinity. In this study, soil complexity was embraced by performing GWAS on natural saline calcareous soil from a coastal Mediterranean region. There is high variation in the mineral nutrient accumulation among different populations within a species depending on the chemical composition, nutrient, and trace element bioavailability from their native soils (Baxter & Dilkes, 2012). Therefore, the natural variation in the ionic profiles of the studied *A. thaliana* accessions was used as the main phenotype for this GWAS.

## RESULTS

Figure S1 details the workflow and the *A. thaliana* accessions and mutants used in each experiment.

### *Arabidopsis thaliana* HapMap performance on saline calcareous soil

A total of 270 accessions constituting the HapMap collection (Horton et al., 2012) were grown for 8 weeks on a saline carbonated soil (SCS) excavated from a coastal region of the northeast of Spain (Figure 1a). The geographical location of

the accessions used in this study and the physicochemical properties of the SCS are described in Figure 1a,b. Selecting an adequate soil to mimic the conditions of representative saline carbonated soils in Mediterranean areas was prioritized. As soil-forming factors and dynamics are interdependent processes that create a unique and high complex system, no commercial soil was considered reliable as a control and plant performance was only assessed on SCS.

High natural variability was observed for rosette diameter (RD) of 8-week-old plants among all the accessions (Table S1). We classified the studied accessions according to their RD into low diameter (LD) and high diameter (HD) groups, based on the 10% tails of the RD normal distribution. Differences in RD were statistically significant among the two groups (Figure 2a).

Elemental profiling of leaf tissue was performed for three plants of each of the 270 studied accessions. High variability was observed depending on the element and the accession (Table S1). To understand the relationship between the elemental concentrations, we performed multivariate correlation analysis on the 10 quantified leaf mineral nutrients and the rosette diameter traits and clustered the elements based on their degree of correlation. The highest positive and negative correlations were found between leaf Fe - Mn ( $R^2 = 0.78$ ) and Fe - K ( $R^2 = 0.64$ ), respectively. Leaf Fe concentrations were strongly correlated to several elements under SCS alkaline salinity conditions besides Mn and K and showed a positive correlation to Ca ( $R^2 = 0.29$ ) and negative correlation to S and P ( $R^2 = 0.27$ ). Although to a less degree, leaf Na displayed significant positive and negative correlations only with Fe ( $R^2 = 0.10$ ) and S ( $R^2 = 0.10$ ). Na and S were the only measured elements showing a significant negative correlation

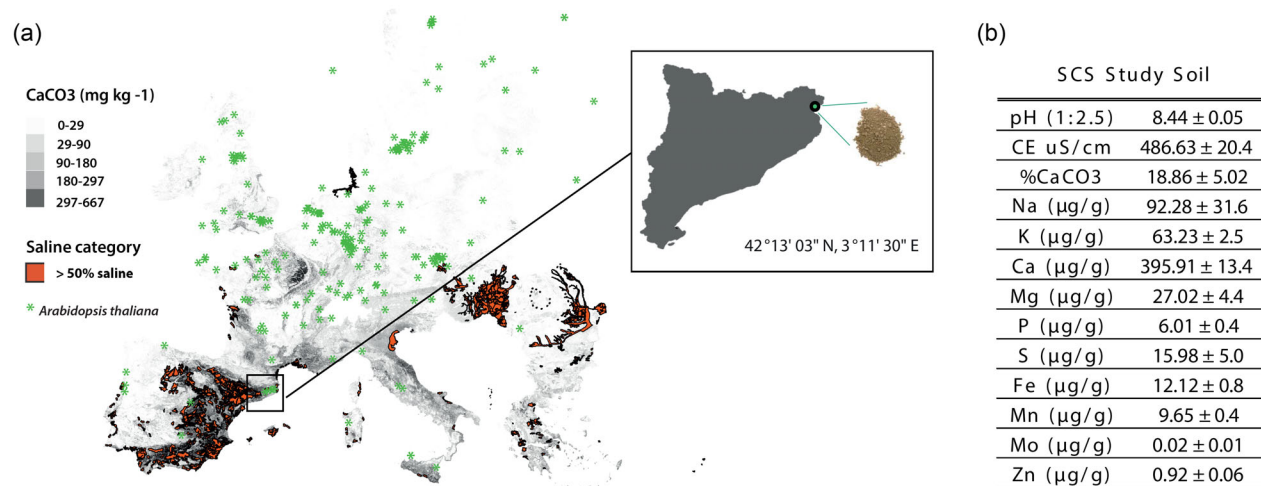


**Figure 1.** Plant material and soil of study. (a) Distribution of saline and calcareous soils in Europe. Green dots indicate the location of origin of the 360 accessions of the HapMap collection. Red area is categorized as saline (>50% surface), and CaCO<sub>3</sub> content (mg kg<sup>-1</sup>) is shown (gray-scale legend). Frame shows the map of Catalunya, indicating the location of the saline calcareous soil (SCS) used in the experiment; (b) physico-chemical characterization of SCS.

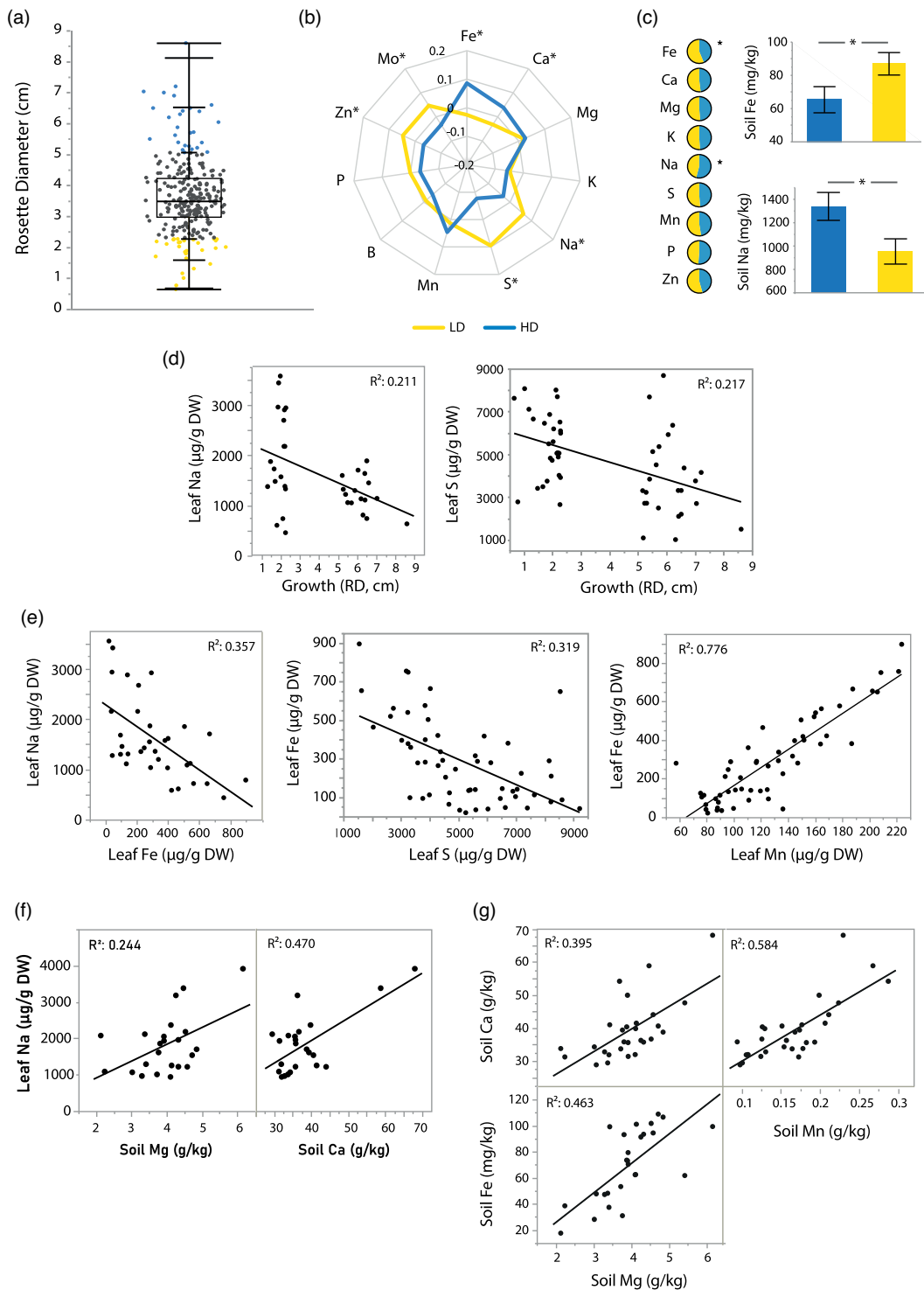


**Figure 2.** Phenotypic analysis of the studied accessions grown on saline calcareous soil (SCS). (a) Scatter plot of the rosette diameter (cm) of all accessions grown on SCS. Each dot represents an accession. Growth categories were established by selecting accessions on the 10% top (blue) and 10% lowest (yellow) rosette diameter. HD: High Diameter group; LD: Low Diameter group; (b) Radial plot with the Z-values of the studied elements in leaves of HD and LD accessions. Axes display Z-scores calculated per element and asterisks show significant differences among the two extreme groups (Student *t*-Test,  $P < 0.05$ ); (c) Chart pie of nutrient content in the native soil of HD (blue) and LD (red) accessions. Asterisks and histograms show the two elements displaying significant differences among the two groups (Student *t*-Test,  $P < 0.05$ ). Plants were grown on SCS for 8 weeks ( $n = 4$ ). (d) Pairwise correlation of leaf mineral nutrients and growth performance (Leaf Na and RD, leaf S and RD, expressed as  $\mu\text{g g}^{-1}$  DW and cm, respectively); (e) Pairwise correlation of Leaf nutrient concentrations (Na and Fe, Fe and S, Fe and Mn, expressed as  $\mu\text{g g}^{-1}$  DW); (f) Pairwise correlation of leaf mineral nutrients and SCS soil element concentrations (Leaf Na and soil Mg and Ca, expressed as  $\mu\text{g g}^{-1}$  DW and  $\text{g Kg}^{-1}$  respectively); (g) Pairwise correlation of SCS soil element concentrations (Ca and Mg, Fe and Mg, Ca and Mn, expressed as  $\text{g Kg}^{-1}$ ). The lines represent the result of linear regression.  $R^2$ : Squared Pearson correlation's coefficient.

with rosette diameter (RD) ( $R^2 = 0.05$ ;  $R^2 = 0.06$ ). Results are represented in the correlogram, clustered heatmap and scatter plot matrix (Figure S3a–c).

Next, leaf element concentrations were compared among the established growth performance groups to further characterize element interactions under SCS and their effects on plant performance. Overall, accessions from both LD and HD (worst and best performance, respectively) showed remarkably different ionic profiles when compared to each other. Individuals from LD had significantly lower Fe concentration and higher leaf Na concentration than individuals from HD. In turn, HD accessions contained significantly less Zn, S and Mo and more Ca than those from LD (Figure 2b). Nutrient ratios with known biological significance in plant growth and nutrition were also assessed in the two groups of accessions. LD plants showed significantly higher Na:K, Mg:Ca, Zn:Fe, S:Fe ratios and significantly lower Fe:Mn ratios than those from the HD group (Figure S2). We confirmed that RD was negatively correlated to leaf Na and S content and, in turn, that the negative correlations between leaf Fe and leaf Na and S were endorsed.

The leaf ionome is largely dependent on the soil nutrient availability. It is well known that geographically widespread *A. thaliana* accessions have evolved mechanisms to balance their nutritional needs based on availability of nutrients in the site of origin (Campos et al., 2021). Thus, we further considered the correlations between the leaf and soil nutrients in the study accessions, and the relations among different soil nutrients at their natural habitats. Leaf Na concentrations correlated positively with concentrations of Mg and Ca in the soil of origin. In turn, high soil Mg and Ca strongly correlated with high soil Fe and Mn, respectively (Figure 2g).

Finally, we analyzed the correlation between RD and leaf elemental profile on SCS and the properties of their soil of origin to further explore the possible relationship between geographic regions and the leaf ionome under alkaline salinity. Estimated soil Na content and other elemental profile data of the native soils of the tested accessions were extracted from public maps of the European Soil Data Centre (ESDAC) (Table S1). As shown, accessions from HD belong to soils with more elevated Na and more limited Fe concentrations than accessions from LD (Figure 2c).

#### Detection of SNPs associated with differential leaf elemental profile on saline calcareous soil

To identify genomic regions underlying the differential growth and ionic responses to alkaline salinity, we conducted GWA analysis on leaf elemental profiles of the accessions grown for 8 weeks on SCS. We identified several significantly associated SNPs using a 25% FDR threshold calculated by the Benjamini-Hochberg procedure. From the 10 phenotypes analyzed, two traits gave significant associations: LNa and LFe (Figure 3). Manhattan plots for

rest of leaf ion concentration phenotypes are provided in Figure S4. A single strong peak of SNPs associated with leaf Na<sup>+</sup> at Chr 4, with the peak centered on *AtHKT1*. Previous QTL mapping and GWAS identified QTLs for leaf Na<sup>+</sup> centered on *AtHKT1* (Baxter et al., 2010; Rus et al., 2006). Such genetic evidence supports that the peaks of SNPs associated with leaf Na<sup>+</sup> and Fe<sup>+</sup> observed in our GWA analysis represent true positive associations and not a false positive caused by high degree of population structure present in *A. thaliana* (Atwell et al., 2010). To account for a possible effect of the *HKT1* locus on the identification of the other loci identified in this GWAs, *HKT1* allelic variations in HD and LD accessions were assessed. The strong *HKT1* variant was confirmed for all accessions used in further analyses. Other significantly associated SNPs [ $-\log_{10}(P) > 6.42$ ; see Methodology] were identified on chromosomes (Chr) 1 (SNP 1) and 4 (SNP 2) for LNa, and on Chr 1 for LFe (SNP 3). A SNP for LNa at Chr 4 with LOD score 5.56 mapping 40 Kb upstream SNP 3 was included in the analyses (SNP 4) for being in moderate LD with SNP 3 ( $R^2 = 0.4$ ), in order not to rule out any potential candidate, as sub-threshold signals with proximity to putative candidate genes have been previously selected to identify novel loci involved in the studied response (Wang et al., 2016). The scores, positions, genes associated with the detected SNPs and genes included in the linkage disequilibrium (LD) regions are detailed in Table S3.

The function and localization of all candidate genes included in the quantitative trait locus (QTL) regions was examined for all described peaks. This led to a total of 22 candidate genes for analysis from which AT4G28900 was a transposable element and discarded. The other 21 genes were selected to identify the causal gene(s) underlying each QTL association to the observed phenotypes.

Among the selected candidates three transporters were found: one mitochondrial transporter, AT1G10680 (*P-glycoprotein 10*, *PGP10*), one cytoplasmic vesicle transporter AT1G10730 (*Adaptor protein-1 mu-adaptin 1*, *AP1M1*) and one Golgi to plasma membrane transporter, AT1G59820 (*Aminophospholipid ATPase 3*, *ALA3*). *PGP10* encodes a P-glycoprotein from the ABC Transporter Family. It associated with differential leaf Na accumulation together with *AP1M1*, which encodes a protein belonging to the clathrin adaptor complex medium subunit family (Qiao et al., 2010). *ALA3* encodes a transporter involved in Golgi to plasma membrane phospholipid transport (Poulsen, López-Marqués, McDowell, Okkeri, Licht, Schulz, & Palmgren, 2008) and associated with differential leaf Fe accumulation.

Another four genes are regulating or involved in kinase activity: one encoding a nuclear kinase inhibitor, AT1G10690 (*Siamese-Related 8*, *SMR8*), one encoding a phosphoribosyl pyrophosphate synthase, AT1G10700 (*Phosphoribosyl pyrophosphate synthase 3*, *PRS3*) and two Casein-Kinase-I-like protein coding genes, AT4G28880

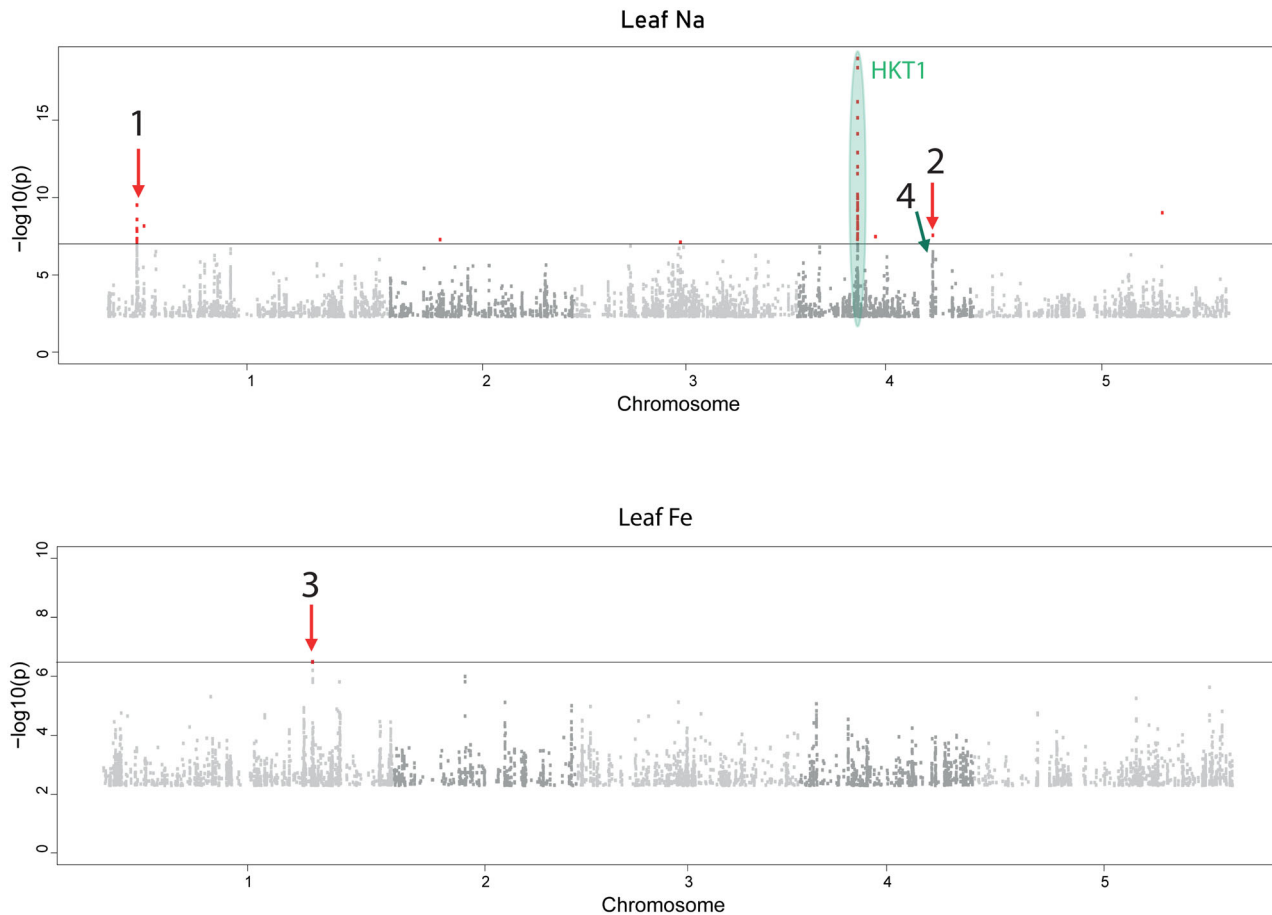


**Figure 3.** Genome wide association studies (GWAS) for leaf ionome traits of HapMap accessions grown on SCS. Manhattan plots displaying the GWAS results for (a) leaf Na concentration and (b) leaf Fe concentration in the studied accessions. The horizontal gray dash-line line corresponds to a nominal 0.05 significance threshold after Benjamini Hochberg (False Discovery Rate) correction. Numbers, red dots and arrows indicate the regions containing the significantly associated locus. Peak of SNPs centered on *HKT1* is circled and labeled. Blue arrow indicates SNP included independently from SNP 3 in the analysis. x-axis: chromosomal position of SNP; y-axis:  $-\log_{10}(P\text{-value})$ . Plants were grown on SCS for 8 weeks ( $n = 4$ ).

(*CKL3*) and AT4G28860 (*CKL4*). All four genes associated with differential leaf Na accumulation. *SMR8* and *PRS3* mapped to Chr1. *CKL3* and *CKL4* mapped to chromosome 4 and both CKL proteins act as signal transducers mainly in the blue light signaling pathway (Tan et al., 2013).

Two genes associated with the two SNPs mapping on Chr 4 for leaf Na accumulation are involved in phytohormone biosynthesis and signaling pathways: AT4G28720 (*YUC8*) and AT4G28910 (*NOVEL INTERACTOR OF JAZ, NINJA*). *YUC8* encodes a member of the flavin-binding monooxygenase family protein, which is involved in auxin biosynthesis and active in the nucleus. The gene is expressed mainly in flowers and shown to be ethylene responsive (Qin et al., 2017). *NINJA* encodes a transcriptional repressor that functions in the jasmonic acid (JA) signaling pathway, has a role in root development, and a key role in leaf development (Pauwels et al., 2010). It is also involved in the adaptive responses to salt stress (Ismail et al., 2014). Two other genes included in the same LD

region as *YUC8* and *NINJA*, are AT4G28730 (*GrxC5*) and AT4G28850 (*ATXTH26*), respectively. *GrxC5* encodes a Glutaredoxin Family Protein with glutathione disulfide oxidoreductase activity. It belongs to the Class I or "Classic" *GRX*'s, which are involved in stress response (Couturier et al., 2011). Specifically, *GrxC5* is present only in Brassicaceae and its dimeric holoprotein incorporates a [2Fe-2S] cluster. *ATXTH26* encodes a xyloglucan endotransglucosylase/hydrolase involved in root growth and cell wall extension (Maris et al., 2009). Another gene with a known biological function in this LD region is AT4G28750 (*PSAE-1*), encoding a protein from the Photosystem I reaction center subunit IV, involved in the response to light stimulus and mRNA binding.

Another gene with promising roles in nutrient homeostasis present in the LD region of SNP 4 associated with differential leaf Fe concentration: AT1G59830 (*Protein phosphatase 2a-1, PP2A-1*). *PP2A-1* encodes a serine/threonine phosphatase, which reverses the actions of protein

kinases. It is a regulator of stomatal development (Bian et al., 2020) and involved in the response to several abiotic stress factors such as heat (Wang et al., 2010), salt (Hu et al., 2017), oxidative stress (Máthé et al., 2019) or drought (Rahikainen et al., 2016).

The other genes included in the analyses have roles in secondary metabolic processes (AT1G10690), cellular lipid metabolism (AT1G10720), homologous chromosome pairing at meiosis (AT1G10710), ubiquitin protein ligase binding (AT1G59800) or are described to encode nuclear proteins (AT4G28890 and AT1G59810), with so far unknown functions.

To verify which of the candidate genes included in the analyses were more likely to be responsible for the observed differential LNa and LFe observed under alkaline salinity conditions, we examined available homozygous T-DNA insertion mutant lines for each gene (Table S4). No seed viability or homozygous lines were obtained for T-DNA insertion lines for AT1G10690 (*SMR8*), AT1G59810 (*AGL50*), AT4G28750 (*PSAE-1*), AT4G28880 (*CKL-3*), AT1G10730 (*AP1M1*) and AT4G28890 (*ATL42*). A total of 12 KO lines were analyzed.

### Mutant phenotyping

The 12 KO lines were grown together with Col-0 (wild type control) on SCS to perform the same phenotyping as conducted with the HapMap studied accessions for the GWAS. In parallel, a plate experiment was performed to observe severity of alkaline salinity effects on seed germination and distinguish this from seed non viability (lines with no germination neither in control nor in treatment conditions). The effects of alkaline salinity conditions on seed germination for all mutant lines and Col-0 and the performance of each line on SCS are shown in Figure 4(a–c). All lines suffered a dramatic inhibition in germination under alkaline salinity conditions (Alk-Sal) (Figure 4a). For both SNPs with the highest associations with LNa on Chr 1 and 4 (SNPs 1 and 3, respectively, at positions 3 562 288 and 14 258 447), the Col-0 reference allele was associated with low LNa. From the candidate genes located in the respective LD regions, *pgp10* (Chr 1), *yuc8* (Chr 4) and *ninja* (Chr 4) accumulated significantly higher leaf Na concentrations on SCS (Figure 4b). For LFe, the Col-0 reference allele for SNP4 on chromosome 1 (located at position 22 010 370) associated with low leaf Fe concentration. Significantly higher leaf Fe was observed in *ala3* when compared to Col-0 (Figure 4c). Growth constraints were observed in all selected lines when compared to WT (Figure 4d).

The selected mutant lines for the candidate genes mapping to differential LNa did not show significant alterations in LFe when compared to Col-0 except for *ninja*, which also displayed reduced LFe ( $P = 0.034$ , Dunnett's Test). Similarly, none of the selected mutants for LFe exhibited an altered LNa phenotype in comparison to WT. This

indicates the trait specificity of each locus association except for AT4G28910 (*NINJA*) (Figure S5).

### Effects of natural allelic variation of the locus of interest in gene expression and plant growth performance under alkaline salinity

To further identify the causal genes underlying SNP associations, HapMap accessions showing extreme phenotypes (ExtP) for the studied traits were selected as "High Leaf Na" (HLNa), "Low Leaf Na" (LLNa), "High Leaf Fe" (HLFe) or "Low Leaf Fe" (LLFe) accessions according to their leaf Na and Fe contents, respectively (Table S5). Plants were re-examined for alkaline-salinity-induced changes in rosette size and ionic profile under hydroponic conditions. The selected ExtP accessions were grown in control and treatment solutions (0.5-strength Hoagland solution at pH 5.7 for control; 40 + 10 mM NaCl + NaHCO<sub>3</sub> at pH 8.3 for the Alk-Sal treatment). Rosette diameter, root length, rosette and root biomass and leaf ionome profiles were assessed after 35 days. Allelic variation at the locus of interest was associated with differential growth (LD, HD) and ionic responses (HLNa/LLNa; HLFe/LLFe) of the studied ExtP accessions. For the locus associated to differential LNa, the alternative variant correlated to the phenotype LD and HLNa (sensitive accession with high leaf Na accumulation) while the common variant correlated to HD, LLNa (tolerant accession with low leaf Na accumulation) (Figure 5a). For the locus associated to differential leaf Fe, LD and LLFe phenotype (sensitive accession with low leaf Fe accumulation) correlated to the common allele variant, while accessions bearing the alternative allele related to HD and HLFe groups (tolerant accession with high leaf Fe accumulation) (Figure 5b).

We measured the expression of the candidate genes in ExtP accessions under control and Alk-Sal hydroponic conditions. Accessions bearing the alternative and common allele variants for each SNP were pooled separately. On the genes surrounding the LNa peak, *PGP10* expression was not significantly different based on this comparison ( $P = 0.89$ , Student *t*-test), while *YUC8* and *NINJA* showed significant differential expression in leaves between accessions from group 1 (bearing the alternative allele) and group 2 (bearing the common allele) ( $P = 0.003$ ,  $P = 0.015$ ,  $P = 0.046$ ; Student *t*-Test). Transcript levels of *PGP10* did not correlate with plant growth ( $R^2 < 0.001$ ) but the relative expressions of *YUC8* and *NINJA* were highly correlated with rosette diameter of each accession under Alk-Sal conditions ( $R^2 = 0.55$ ;  $R^2 = 0.50$  and  $R^2 = 0.42$ , coefficient of determination of the pairwise correlation) (Figure 6a). For LFe peak, differences in *ALA3* expression were not found in shoots (Figure 6b) but roots (Figure 8b) ( $P = 0.0002$ ) and gene expression levels correlated positively with plant performance under Alk-Sal conditions ( $R^2 = 0.45$ ;  $R^2 = 0.30$ , respectively) (Figure 8b).

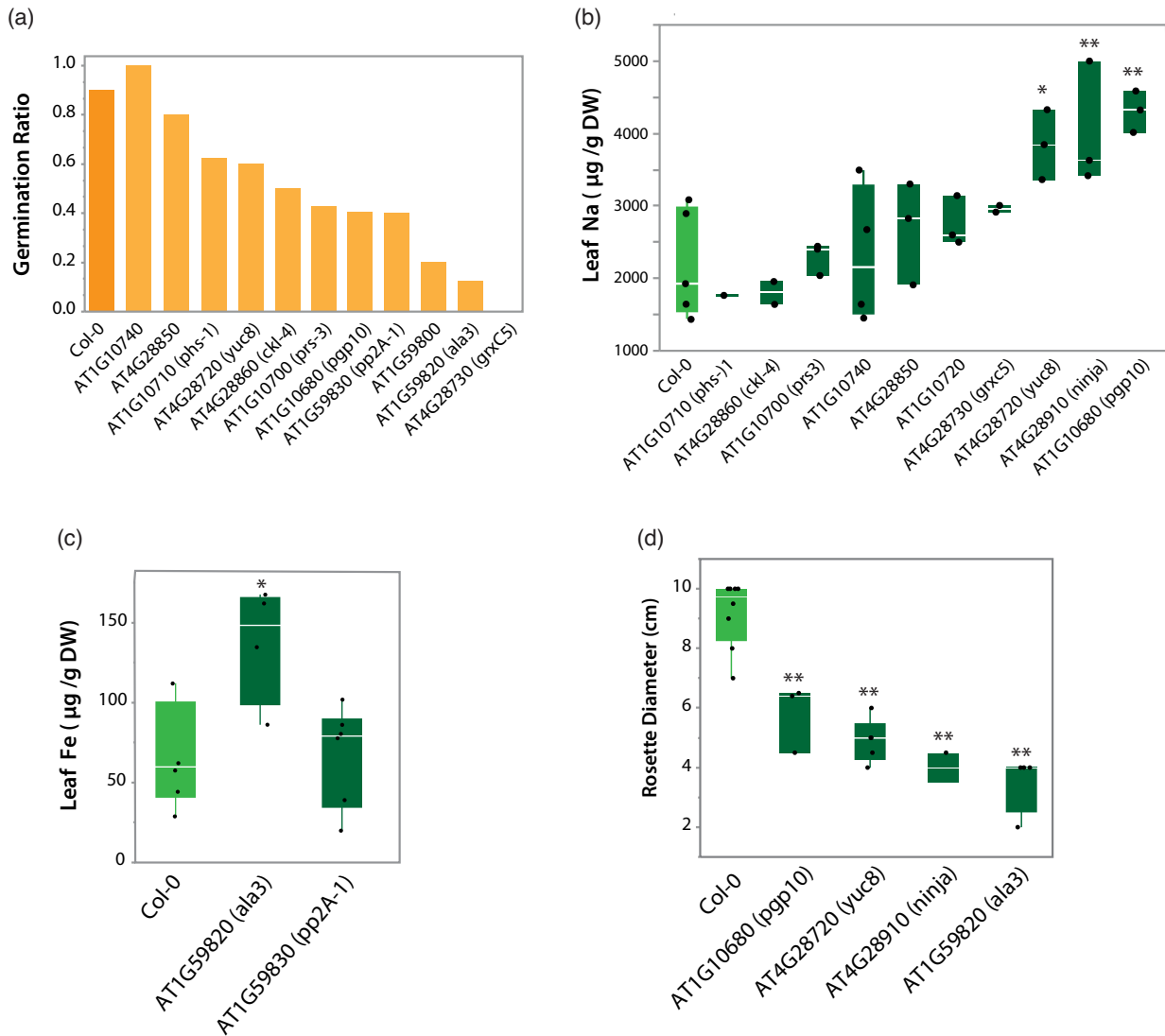


**Figure 4.** Phenotyping of T-DNA insertion mutants for the identified candidate genes. (a) Seed germination on plates under control and treatment conditions. Germination rate [(% Germination – Treatment)/(% Germination – Control)] of T-DNA and Col-0 lines. Plants were grown on agar plates for 1 week in control (½ MS at pH 5.9) or bicarbonate (½ MS at pH 8.3 and 10 mM NaHCO<sub>3</sub>) treatment conditions. *n* = 10 plants per accession and treatment. Mean ± SE of leaf Na (b), and leaf Fe concentration (µg g<sup>-1</sup> DW) (c) and Rosette Diameter (cm) (d). Asterisks indicate significant differences between mutant and Col-0 wild type (\**P* < 0.05; \*\**P* < 0.01, Dunnett's test). Plants were grown on SCS for 8 weeks (*n* = up to 6 plants per accession and treatment).

### Causal polymorphisms at the NINJA, YUC8 and ALA3 locus

After observing that allelic variation at the pinpointed candidates is causal for the differential gene expression level and ultimately for the differential response to alkaline salinity in the study accessions, the identification of most causal sequence polymorphisms was addressed by conducting haplotype analysis on a 50-kb region centered on each candidate gene. The pattern of polymorphisms of different haplotypes that associated with contrasted phenotypes was compared by the analysis of SNPs in intermediate ( $R^2 > 0.6$ ) and high LD ( $R^2 > 0.8$ ) with the GWAS marker SNP.

Three splice variants are associated to the *NINJA* locus. AT4G28910.1 and AT4G28910.2 are 2753 bp, while AT4G28910.3 is 207 bp shorter (2546 bp). The haplotypes of the accessions with highest leaf Na – bearing the alternative allele of the marker SNP – and accessions with lowest leaf Na – possessing the non-reference allele at the marker SNP – exhibit 5 SNPs: one in the 3' UTR, 2 in the first intron for all 3 variants, 1 in the first intron of variant 1 but within the splice region of variants 2 and 3, and one in the first intron of variants 1 and 2 but within the splice region of variant 3. *YUC8* is 1734 bp long with one exon. Three SNPs in LD with the marker SNP surrounding the



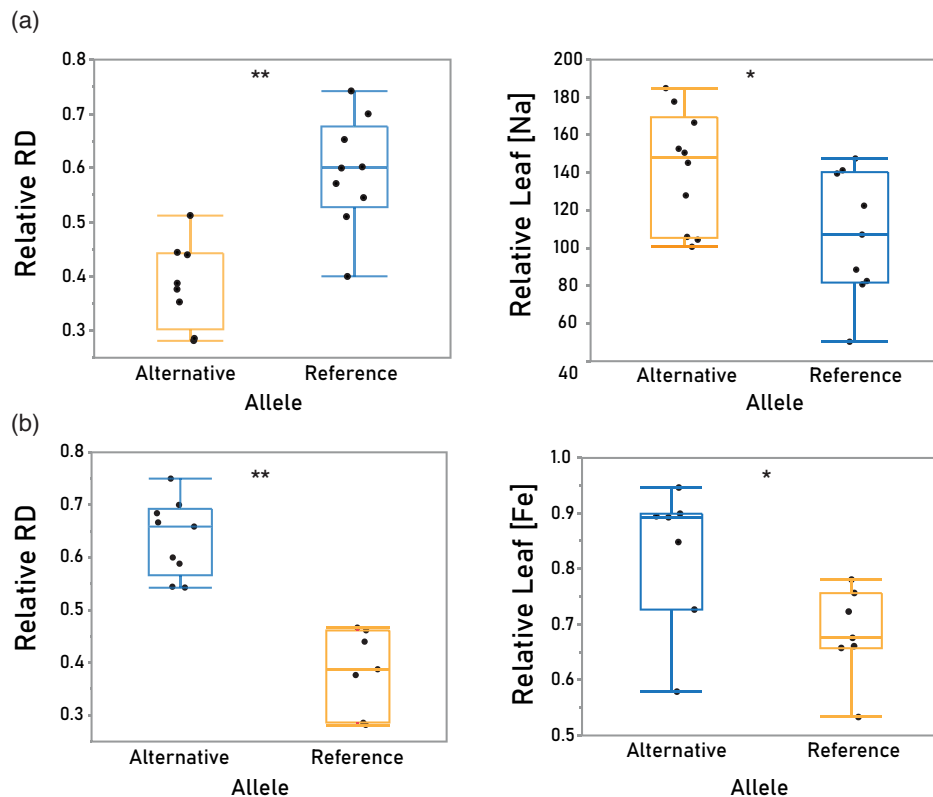


**Figure 5.** Phenotyping of selected accessions displaying extreme phenotypes and contrasted alleles for each SNP of interest under hydroponic conditions. From left to right, mean  $\pm$  SE of relative rosette diameter (Relative RD) per allele variant and relative leaf element concentration per allele variant for all LNa (a) and LFe (b) SNPs. Each dot represents 1 individual. Color boxes indicate advantageous (blue) and detrimental (yellow) alleles for each SNP. Plants treated with 0 or 40 mM NaCl + 10 mM NaHCO<sub>3</sub> (pH 8.3) for 2 weeks. Three populations with up to 3 plants per population were pooled per each group. Asterisks indicate significant differences (\* $P$  < 0.05; \*\* $P$  < 0.01, Student  $t$ -Test).

*YUC8* coding region were found at the upstream, exon and downstream *YUC8* region. The exonic SNP is a synonymous variant. *ALA3* is a 9083-bp gene. Haplotypes of the accessions with highest leaf Fe – bearing the reference allele of the marker SNP – and accessions with lowest leaf Fe – possessing the alternative allele at the marker SNP – exhibit 4 SNPs: 970 bp upstream the gene coding region, 2 at the promoter region (639 and 529 bp upstream the coding region) and 1 at the third intron.

SNP polymorphisms around the *NINJA*, *YUC8* and *ALA3* locus and SNPs differing from the Col-0 reference genome sequence are shown in Figure 7(a–c).

#### Identified novel loci are not masked by effects of known major players in Na and Fe homeostasis

To assess if expression patterns in the pinpointed candidate genes are determined by expression patterns of known major players in salinity and alkalinity tolerance, the expression levels of *HKT1* and *SOS1* (for the leaf Na SNP) and *FRO2* and *IRT1* (for the leaf Fe SNP) were analyzed in ExtP root samples. *YUC8*, *NINJA* (leaf Na SNP) and *ALA3* (leaf Fe SNP) were included. *SOS1* and *YUC8* did not show differences in root expression levels when

comparing the two ExtP pools, while *NINJA* displayed significantly enhanced expression in the ExtP pool bearing the alternative allele ( $P = 0.003$ , Figure 8a). *HKT1* followed the same trend and its expression level increased significantly, but these differences were not caused by effects of *HKT1* allelic variation in the ExtP pools, as all used accessions were confirmed to carry the *HKT1* reference (*HLS*, Col-0 -type) allele (Table S5). Root *IRT1* and *FRO2* did not show expression differences according to the study group classification, while *ALA3* expression levels were dramatically increased in ExtP accessions bearing the alternative allele ( $P = 0.0003$ , Figure 8b).

## DISCUSSION

### Natural variation in the response of *Arabidopsis thaliana* HapMap accessions to alkaline salinity

In this study, growth and nutritional status in a set of 270 natural accessions of *A. thaliana* were screened under a natural saline-carbonate soil and the molecular genetic mechanisms underlying stress responses to alkaline salinity were explored by conducting GWAS. Among all accessions surviving to the end of the experiment, two groups

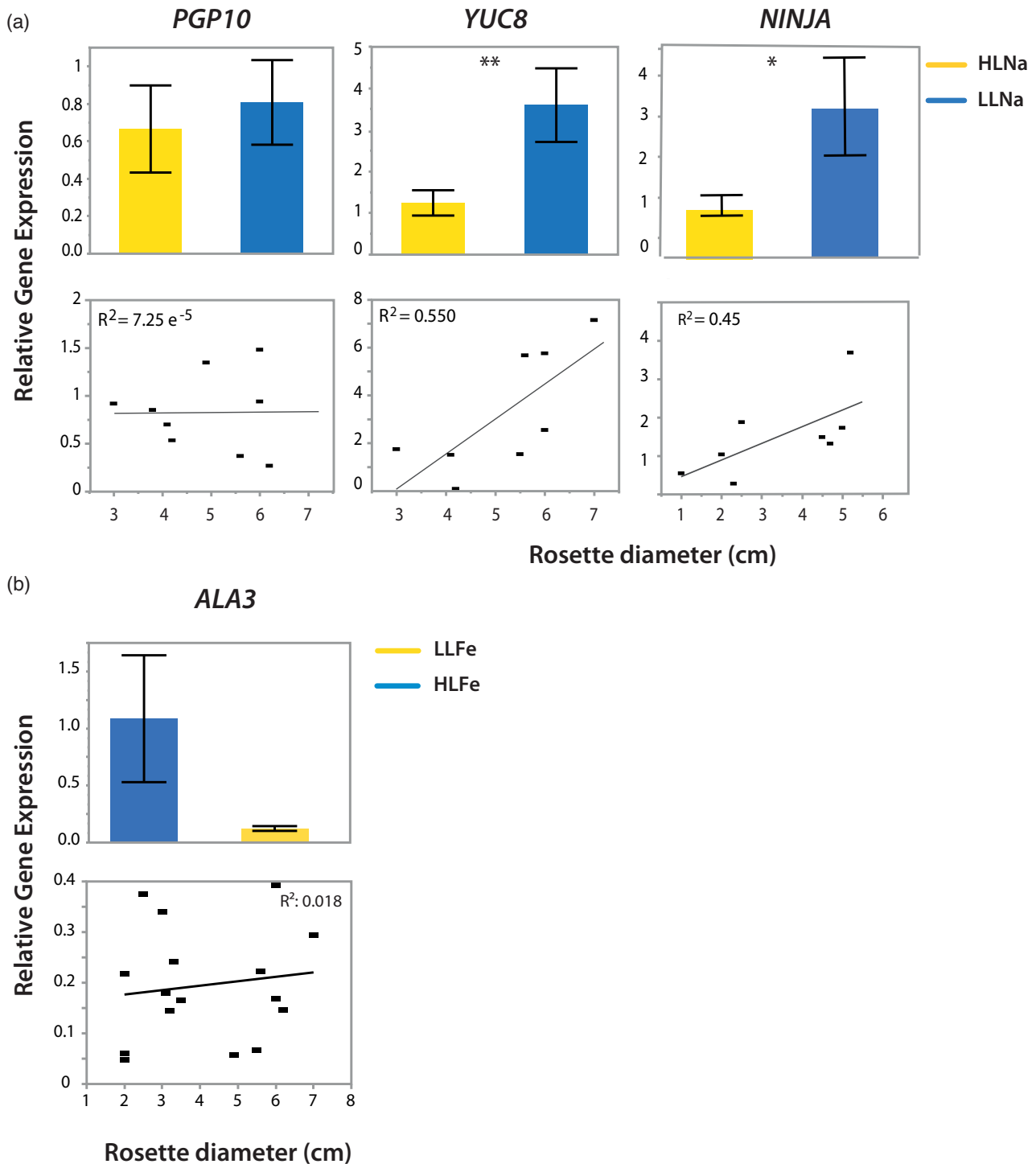


**Figure 6.** Effects of allelic variation of selected candidate genes in gene expression levels. From left to right, gene expression of *PGP10*, *YUC8* and *NINJA* (a) and *ALA3* (b) in selected natural populations displaying extreme LNa and LFe phenotypes and contrasted alleles (ExtP). Scatter plots of relative gene expression (y-axis) and plant rosette diameter (x-axis) are represented below each gene expression plot. The lines represent the result of linear regression.  $R^2$ : Squared Pearson correlation's coefficient. Expression levels were normalized to expression in Col-0. Error bars: SE Leaf and root samples of 3 populations with 3 plants per population were pooled per each group. Populations used are listed in Table S5. Data from three independent biological replicates each with two technical replicates are analyzed. Asterisks indicate significant differences (\* $P < 0.05$ ; \*\* $P < 0.01$ , Student  $t$ -Test).

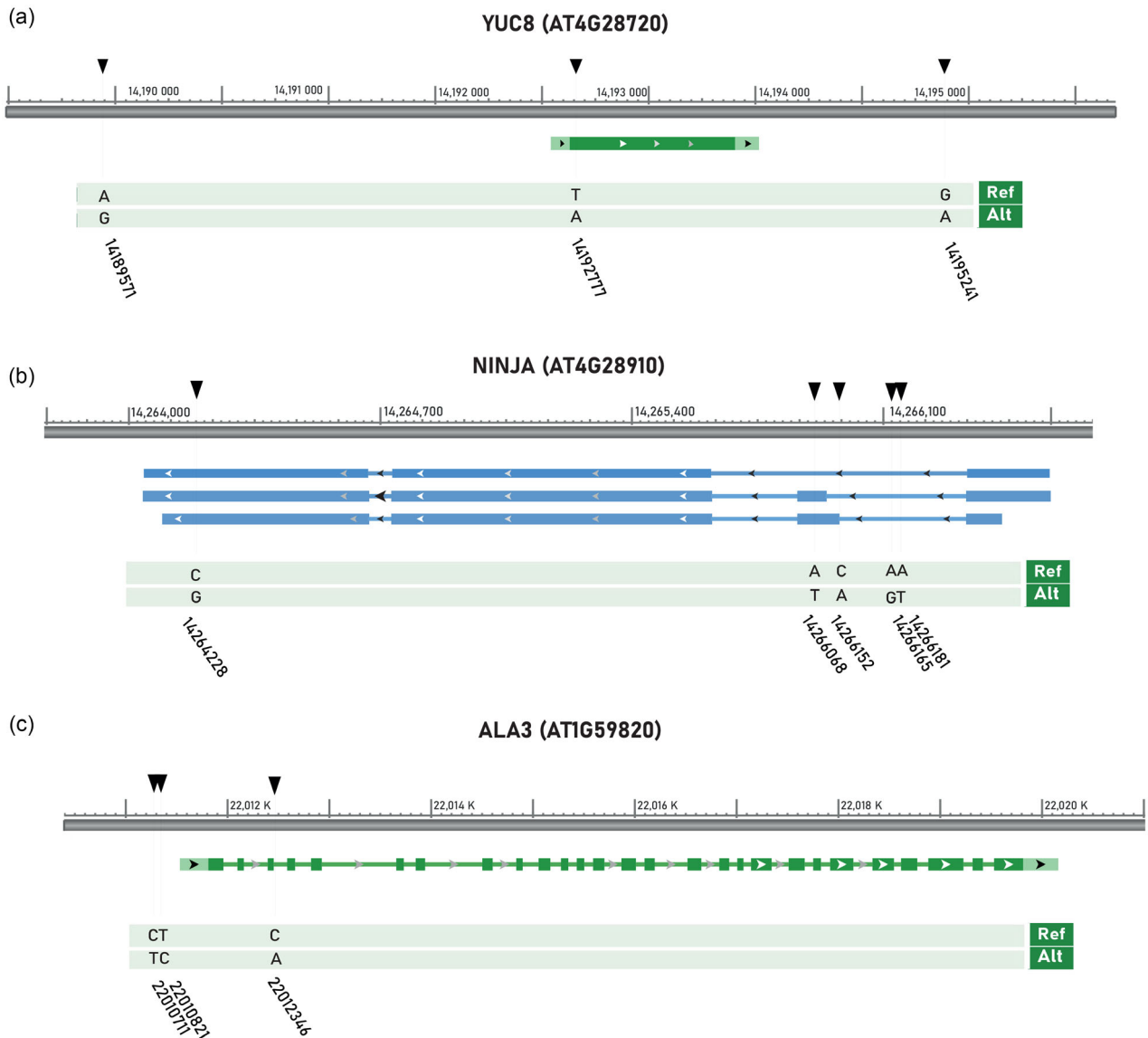


**Figure 7.** SNP polymorphisms surrounding the NINJA, YUC8 and ALA3 locus. Black triangles and orange lines: most likely candidate SNPs underlying the allelic effects. Gene orientation is indicated with an arrow on the right (a, c) and left (b). Exons are indicated with yellow boxes and introns with lines connecting them. Splice variants are shown when present. Reference and alternative allele nucleotide changes and SNP position are marked below; chromosome positions are indicated at the top (picture from <https://www.arabidopsis.org/index.jsp>).

were established: LD accessions (Low Diameter – plants below the 10% quartile), with poor adaptation to SCS and HD accessions (High Diameter – plants above the 90% quartile), with good adaptation to SCS. Differences in leaf nutrition, allelic variants of final candidate genes and differential gene expression levels between HD and LD groups under alkaline salinity are discussed.

**Footprint of eco-geographical adaptation in the ionic profiles of *A. thaliana* natural populations**

High natural variation in the ionic profiles of the 270 *A. thaliana* accessions was observed, in accordance with the

high biodiversity in the mineral nutrient accumulation known to exist among different populations within a species reflecting the chemical composition, and the nutrient and trace element bioavailability from their native soils (Baxter & Dilkes, 2012). The *A. thaliana* HapMap set of natural accessions comes from habitats with a broad range of soil physicochemical parameters, including Na, Fe and CaCO<sub>3</sub> concentrations. Using a geographically widely distributed collection of accessions offers the opportunity of identifying causal genetic variants important for local adaptation, including those constituting adaptation to a combined stress like alkaline salinity (Miller & Busch, 2021).

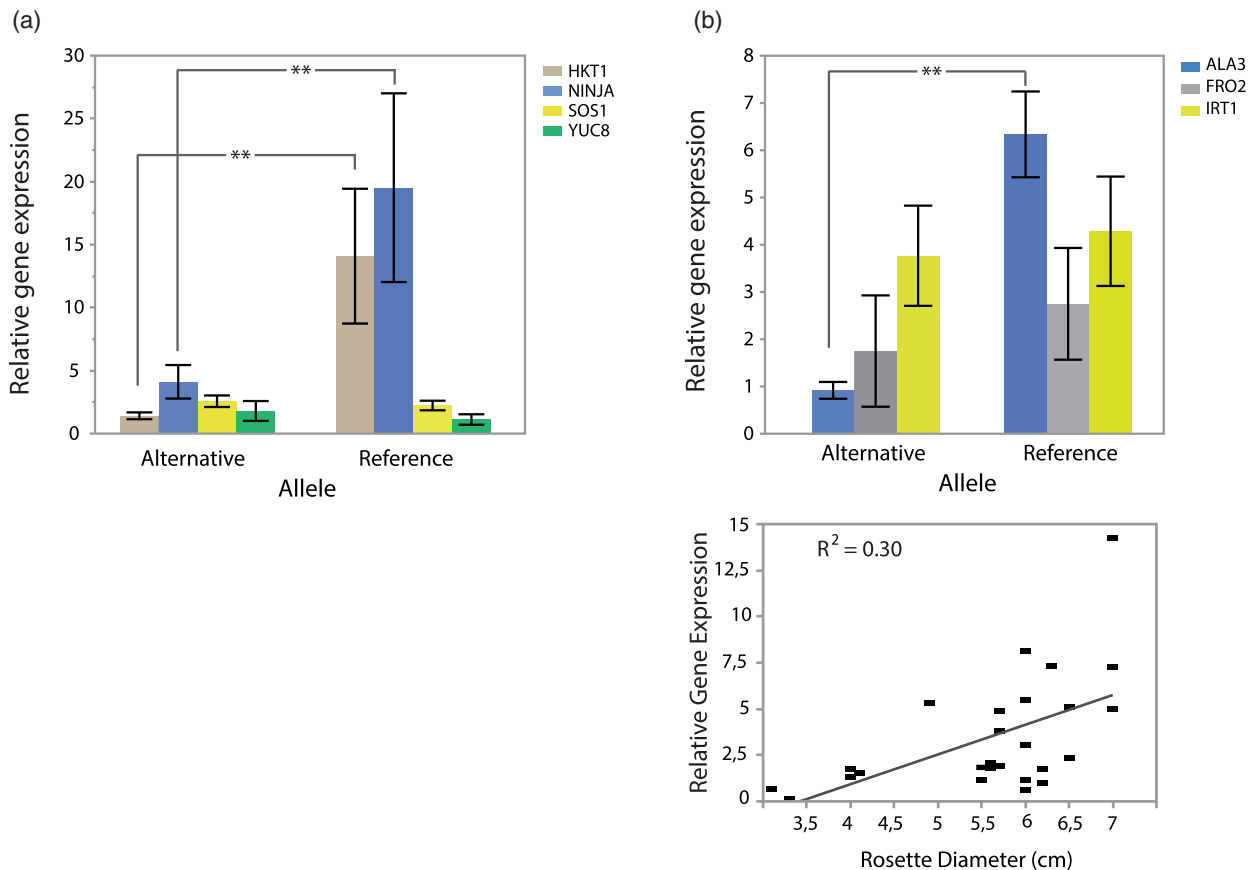


**Figure 8.** Expression pattern of major players in salinity and iron deficiency in roots of ExtP accessions. Gene expression of *NINJA*, *YUC8*, *HKT1* and *SOS1* (a) and *ALA3*, *IRT1* and *FRO2* (b) in roots of ExtP accessions. Scatter plots of relative gene expression (y-axis) and plant rosette diameter (x-axis) are represented below *ALA3* gene expression plot. The lines represent the result of linear regression.  $R^2$ : Squared Pearson correlation's coefficient. Expression levels were normalized to expression in Col-0. Error bars: SE Root samples of three accessions with three plants per accession were pooled per each group. Populations used are listed in Table S5. Data from three independent biological replicates each with two technical replicates are analyzed. Letters a and b indicate significant differences between mRNA expression levels ( $P < 0.05$ , HSD Tukey).

We noticed that HD accessions originate from sites with higher Na and lower Fe soil concentrations. As expected for poorly adapted accessions, when grown on SCS LD plants display higher leaf Na and lower leaf Fe concentrations than HD plants. SCS study soil has an average EC of  $487 \mu\text{S cm}^{-1}$ , pH above 8 and an average  $\text{CaCO}_3$  concentration of 19%. Thus, it is classified as moderately saline (Fan et al., 2011) and calcareous (de Santiago-Martin et al., 2013; Terés, 2017). In arid and semiarid climates, high evapotranspiration rates move soluble  $\text{Na}^+$ ,  $\text{Ca}^{2+}$ ,  $\text{Mg}^{2+}$ ,  $\text{K}^+$ ,  $\text{CO}_3^{2-}$  and  $\text{HCO}_3^-$  ions to the superficial soil layers leading to the co-occurrence of alkaline-saline soils, which are estimated to cover 831 million hectares of Earth (FAO, 1973). In this context, Fe uptake efficiency is critical to prevent chlorosis under conditions of high soil pH (Hsieh & Waters, 2016) and salinity aggravates this problem by negatively affecting the acquisition and internal use of Fe by plants (Ben Abdallah et al., 2017; Rabhi et al., 2007; Zhou et al., 2017). The observed results point to the presence of a footprint of eco-geographical adaptation to alkaline

saline soils in the study accessions, where not only a reduction in Na uptake or an enhancement in Na compartmentalization (Volkmar et al., 1998), but also an efficient acquisition of iron is advantageous (Li et al., 2016; Yousefi et al., 2007). Altogether it suggests that the enhanced response of HD plants to SCS is shaped by alkaline salinity fitness promoting trade-offs.

HD accessions displayed lower Na:K under SCS when compared to LD individuals. It has been proven that alkaline salinity has a larger effect on the rice root Na:K ratio than salinity alone (Shi & Sheng, 2005). This indicates that maintaining a low Na:K ratio in response to alkaline salinity is a main mechanism of ion homeostasis regulation, as it is for salinity alone (Hu et al., 2022).

The HD group also showed significantly better Fe-S adjustment, as the decreased leaf Fe accumulation in LD accessions was accompanied by a strong increase in leaf S concentration. There is dynamic crosstalk between plant Fe and S networks, which is reported to be critical under low Fe availability (Hantzis et al., 2018) but also under S

deficiency (Ostaszewska et al., 2014; Vigani & Briat, 2016). Here, maintenance of Fe:S is favoring HD individuals under SCS likely by optimizing Iron–sulfur (Fe–S) clusters, which are at the center of photosynthesis, respiration, amino acid, and DNA metabolism (Mendoza-Cózatl et al., 2019). Iron–sulfur clusters are also required for most molybdo-enzymes to function (Bittner, 2014). HD accessions showed significantly lower leaf Mo accumulation. Molybdenum is a primary mineral nutrient highly available in alkaline soils which can interfere with Fe acquisition when present in high concentrations (Alloway, 2013). Mo levels of the study accessions on SCS (2–380  $\mu\text{g g}^{-1}$ ) are much larger than what was found for shoot Mo concentration ranges (0.7–50  $\mu\text{g g}^{-1}$ ) in *A. thaliana* accessions grown in potting mix or hydroponics (Baxter et al., 2008). Thus, an adjustment in Mo accumulation may favor, among others, Fe nutrition in HD accessions, which in turn maintains Fe:S ratios and ultimately Mo co-factor (Moco) biosynthetic activity (Teschner et al., 2010).

We observe significantly higher leaf Ca accumulation in HD accessions (Figure 2b). Interaction between salinity and Ca seems to play a pivotal role in the overall performance of the studied accessions: higher Ca concentrations under salinity inhibit  $\text{Na}^+$ -induced  $\text{K}^+$  efflux by counteracting the plasma membrane (PM) depolarization induced by salt stress and thereby increase  $\text{K}^+$  absorption (Bacha et al., 2015; Shabala et al., 2006). In turn, high Ca levels in calcareous soils can alter Mg uptake and induce Mg deficiency in plants (Mengel & Kirkby, 2001; Shaul, 2002), as Mg and Ca are strongly antagonistic (Voogt 1988). Our results suggest that enhancing Ca nutrition - resulting in a decrease in the Na:Ca ratio and an increase of K content -, rather than maintaining low Ca:Mg ratios to avoid Mg deficiency, favors plant performance under alkaline salinity.

HD accessions accumulated significantly less Zn than LD accessions on SCS. Both high soil carbonate/bicarbonate and high Na affect Zn availability (Akhtar et al., 2019) and our data show a significant negative correlation between RD and leaf Zn concentration (Figure S3b). However, plants generally exhibit Zn deficiency symptoms at shoot concentrations below 15–20  $\mu\text{g g}^{-1}$  (Babu et al., 2014) and HD accessions display higher average Zn concentration in leaf on SCS (73  $\mu\text{g g}^{-1}$ ). Moreover, Fe:Zn ratios are significantly higher in HD accessions. Crosstalk in Zn and Fe nutrition has been extensively reviewed (Pineau et al., 2012; Rai et al., 2021). Several Zn membrane transporters (mainly IRT-like proteins) are regulated by Fe status and can transport both Fe and Zn (Shanmugam et al., 2013; Vert et al., 2001; Yuan et al., 2008). Here, the enhanced Fe accumulation lead by alkalinity in HD plants could be related to the observed decrease in leaf Zn concentration in these accessions and thus be a tolerance mechanism on SCS. These results are in line with previous studies in which Zn deficiency led to increased Fe

accumulation in bean (Cakmak, 2000) and, in the opposite trend, iron deficiency led to Zn excess in maize (Akhtar et al., 2019).

HD accessions displayed significantly higher Fe:Mn ratio than LD accessions under SCS. Plants grown in SCS showed Fe:Mn ratios ranging from 0.8 to 4. From the 12 study accessions displaying Fe:Mn ratio below 1.5, 8 belonged to LD group. On the opposite trend, 15 out of 20 accessions showing Fe:Mn ratio above 2 were from HD group. Classically, the optimum Fe:Mn ratio in plants has been given as 1.5–2.5 (Shive, 1941). It is well established that Fe, Mn and other divalent ions share transporters (e.g. IRT1) and that Fe-dependent chlorosis in *A. thaliana* can be alleviated by means of sequestration of Mn in root vacuoles (Eroglu et al., 2016). Thus, HD accessions might be more able to adjust Fe:Mn homeostasis by reducing Mn root-to-shoot translocation (Milner et al., 2013) or increasing Mn import into root vacuoles (Li et al., 2019) leading to increased Fe:Mn ratios under SCS.

#### Detection of SNPs associated with differential leaf elemental profile on saline calcareous soil

In this study, we report significant natural variation of leaf Na (LNa) and Fe (LFe) content in a panel of 270 *Arabidopsis* natural populations exposed to saline carbonated soil. We identified allelic variation in *NINJA* and *YUC8* genes to be likely causal for the variation in leaf sodium concentration (LNa) and in *ALA3* for the variation in leaf iron concentration (LFe).

Allelic variation in these genes leads to changes in their mRNA expression and is not associated to allelic variation in the main genes responsible for differential plant responses to either salinity (*HKT1*, *SOS1*) or alkalinity (*IRT1*, *FRO2*).

Two out of the five SNPs detected in the *NINJA* gene are splice-site mutations - as they are found within splice sites (the boundary of an exon and an intron) in one or more *NINJA* splice variants. Both SNPs emerge as the top candidates contributing to genotype-specific splicing events under alkaline salinity at the *NINJA* locus, as alternative splicing (AS) regulates transcript levels (Grodecká et al., 2017) and contributes to plant adaptation to their environment (Syed et al., 2012). One SNP in *YUC8* causes an exonic synonymous variant. Far from having no effects on the synthesized protein, coding synonymous variants can have a significant impact on mRNA structure, translation rate and expression (Edwards et al., 2012). *ALA3* contains 2 of the 4 assessed SNPs in the promoter region, which have a high potential to alter gene expression for being close to transcription start sites (Greenbaum & Deng, 2017). The rest of potentially causal SNPs are in non-coding intragenic regions (Figure 8) and therefore they do not have an obvious impact on gene expression or protein conformation (Robert & Pelletier, 2018). Still, they

might be good indicators for the leaf Na and Fe accumulation phenotypes and for the expression level changes detected in the proximal genes. This suggests that *YUC8*, *NINJA*, and *ALA3* could be genes under selection and might be affected by structural variation that should be further explored.

*NINJA* (AT4G28910, Novel interactor of JAZ) acts as a transcriptional repressor and is a negative regulator of jasmonate responses. *NINJA* interaction with JAZ proteins (jasmonate ZIM-domain repressor proteins) has been experimentally determined. In turn, *MYC2* interacts physically with JAZ proteins, thus regulating JA-Ile-responsive gene expression. JA-Ile is a plant hormone that regulates a broad array of plant defense and developmental processes (Pauwels et al., 2010). Transcriptomic analysis has revealed the importance of JA-Ile in the response of *A. thaliana* plants to overcome moderate saline stress (Erice et al., 2017).

*YUC8* (AT4G28720) is an auxin biosynthetic gene and *yuc8* mutants (null mutants of *YUC8*) have previously been shown to suffer reduction in hypocotyl and petiole length under both high and low red to far-red (R:FR) conditions. We showed that the *yuc8* line developed significantly smaller rosette, shorter roots and higher leaf Na accumulation under alkaline salinity conditions when compared to WT plants. It has been hypothesized that down-regulation of auxin signaling might be part of *A. thaliana* acclimation to neutral salinity (Iglesias et al., 2014). More recent studies have shown that exogenous auxin application alters sodium ion accumulation and plays a protective role in salinity challenged strawberry (Zhang et al., 2021). Furthermore, a link between enhanced auxin accumulation mediated by *YUCCA* genes and a better developed root system architecture for the acquisition of salinity stress tolerance has been hypothesized in rice (Saini et al., 2021). Several auxin biosynthetic genes have been reported as direct targets of *YUC8*: *AUF1*, *TAA1*, *TAR1*, *TAR2*, shown to regulate local auxin biosynthesis in primary root tips (Ursache et al., 2014).

The jasmonic acid signaling pathway has shown to be linked to auxin homeostasis through the modulation of *YUC8*, and roots of *yuc8* and *yuc9* knockout mutants displayed a reduced response to methyl jasmonate (MeJA) (Hentrich et al., 2013). Phytohormones modulate a wide range of responses during the whole plant life cycle and the alteration of endogenous phytohormonal levels is a key factor for the regulation of plant growth and reproductive responses to environmental stimuli. Here we suggest a role of *YUC8* and *NINJA* expression levels in the regulation of auxin and jasmonic signaling pathways thus affecting plant tolerance to alkaline salinity. Quantification of endogenous phytohormone concentrations and expression levels of direct targets of *YUC8* and *NINJA* knockout and overexpressing lines grown on alkaline salinity stress will

help to confirm its involvement in tolerance acquisition to saline calcareousness in the soil and to elucidate their mechanism of action and possible mutual interaction.

*AtALA3* encodes a phospholipid translocase active in plasma membrane and the trans Golgi network. It has been reported to be important for vegetative growth and reproductive success in *A. thaliana*. Screening of *ala3* knockout mutants showed that *ala3* was growth-defective dependent upon both temperature and soil when compared to Col-0 (McDowell et al., 2013). *ALA3* contributes to secretory vesicle formation by assisting in the formation of slime vesicles in root tip cells (Poulsen, López-Marqués, McDowell, Okkeri, Licht, Schulz, Pomorski, et al., 2008) and helps regulate polar growth by controlling phosphatidylserine exposure at the plasma membrane cytoplasmic face (López-Marqués et al., 2021). Physical interaction between *AtALA3* and two ARFGEFs (ADPribosylation factor GTPases) - *BIG3* (Brefeldin A-Inhibited Guanine Nucleotide-Exchange Protein3) and *GNOM*, which is essential for proper trafficking of PIN auxin transporters – has been observed in endomembrane, thus regulating trafficking events in the late secretory pathway and *ala3* mutants are defective in auxin mediated developmental processes (Zhang et al., 2020). There is increasing evidence for a role of auxin in plant response to both the Fe deficiency (Celletti et al., 2020) and salinity (Cackett et al., 2022). Plant P4 ATPases are expected to have a major role in any physiological process involving lipid signaling, vesicle formation and/or lipid-dependent protein recruitment to membranes. Plants sense environmental stimuli and transduce the signal into downstream biological responses often through the plasma membrane, which is the interface between the cell and the environment and the source for signaling lipids. Salinity is well known to change membrane lipid composition in plants, and to alter membrane permeability for water, ions, and metabolites (Tsydendambaev et al., 2013). Moreover, membrane lipids are directly affected by pH, due to their acid-basic properties. The assessment of the effects of an *ALA3* hyper-functional allele in membrane fluidity and permeability, regulation of lipid-dependent signaling cascades and control of other gene clusters that might activate plant adaptation under alkaline salinity should be addressed using loss of function, homozygous knockout, and overexpressing mutant lines for *ALA3*.

Altogether, we demonstrate Na-Fe homeostasis are key features in the adaptation of *A. thaliana* to saline alkaline conditions. Our GWAS approach using a saline calcareous natural soil allowed the identification of new players in this crucial ion homeostasis regulation: *YUC8* and *NINJA* associated with Na leaf exclusion (providing a low leaf Na phenotype) and *ALA3* with high Fe leaf accumulation. The importance of these genes for tolerance to saline alkaline conditions is further highlighted by the fact

that, excepting *HKT-1*, for which absence of allelic variation in the study accessions has been confirmed, the study populations bearing alternative and common allelic variants for each identified locus do not differ in the expression of well-established genes involved in Na and Fe homeostasis such as *SOS1*, *FRO1* and *IRT1*. Recent studies have shown that accessions with tolerance to moderate salinity regulate Na:K ratios under salinity by enhancing *HKT1* expression in roots but are unable to increase *HKT1* root expression under alkaline salinity (Pérez-Martín et al., 2022). This suggests that mechanisms for a better maintenance of Na:K balance under salinity conditions are likely to differ from those under alkaline salinity and that the latter need to be better understood.

## EXPERIMENTAL PROCEDURES

### HapMap phenotyping and GIS data extrapolation

Seeds of the *Arabidopsis thaliana* HapMap cohort (354 natural accessions) were obtained from Nottingham *A. thaliana* Stock Centre (NASC, Nottingham, United Kingdom). The list and information of the accessions is detailed in Dataset S1. Seeds were surface sterilized using 5% sodium hypochlorite (NaOCl) solution under constant agitation for 10 min and rinsed with sterile water six times. Seeds were stratified for 4 days at 4°C after sowing to synchronize germination, then four seeds per accession were sown in saline-carbonated soil (SCS) into Aratrays of 51 individual pots especially suited for *A. thaliana* ([www.arasystem.com](http://www.arasystem.com)). The SCS used for treatment was a mix of soil originating from a parcel of natural saline-carbonated soil in L'Escala, NE Catalunya, Spain (42°13'03"N 3°11'30"E) and perlite (3:1). The SCS had previously been characterized as suitable for saline-carbonate stress analysis (Table S1) (Pérez-Martín, 2020). Aratrays were placed in a growth chamber with 150  $\mu\text{mol m}^{-2} \text{sec}^{-1}$  of PAR, 10 h light/14 h dark photoperiod, and 25°C/20°C day/night temperature. Trays were bottom-watered twice weekly with deionized water with no further nutrients added and aratrays were rotated horizontally to help reduce gradient effects for light, temperature, and humidity.

Germination and seedling survival were monitored. Fifty-five-days old plants were harvested to measure their nutrient mineral contents and Rosette Diameter (RD), Rosette Leaf Area (RLA) and Fresh Weight (FW) of three individuals per accession were measured at the end of the experiment.

To estimate the edaphic parameters of the native soil of each *A. thaliana* accession, location coordinates and public maps from the European Soil Data Centre (ESDAC) database (Panagos et al., 2012) were combined using Q-GIS1. Natural accession coordinates were extracted from GWAPP2 in WGS84 system (latitude and longitude). Maps of soil properties at European scale, based on Lucas, 2009/2012 topsoil data from the European Soil Data Centre (ESDAC) were used to extract the following variables: pH (measured in H<sub>2</sub>O), pH (in CaCl<sub>2</sub> 0.01 M solution), Cation Exchange Capacity (CEC), Calcium carbonates (CaCO<sub>3</sub>), C:N ratio, and N, P, and K concentrations (mg kg<sup>-1</sup>).

### Elemental composition of soils and plants

To analyze the composition of the SCS, six independent samples from the trays used for the pot experiment (three at the beginning and three at the end of the experiment) were collected. The soil characterization was performed on the 2-mm fraction samples

following the extraction method described by Busoms et al. (2018). Plant tissues were sampled by removing 2–3 leaves (1–5 mg dry weight) and washing them with 18 milli-Q water before being placed in Pyrex digestion tubes. Sampled plant material was dried for 2 days at 60°C and weighed before open-air digestion in Pyrex tubes using 0.7 ml concentrated HNO<sub>3</sub> at 110°C for 5 h in a hot-block digestion system (SC154-54-Well Hot Block, Environmental Express, Charleston, SC, USA). Concentrations of the selected elements (Fe, Ca, K, Mg, S, Na, P, Mn, Mo, Cu, B, Zn and Ni) were determined by ICP-MS (Perkin Elmer Inc., ELAN 6000, MA, USA) or ICP-OES (Thermo Jarrell-Ash, model 61 E Polyscan, England).

### GWA studies and candidate genes selection

Genome Wide Association Studies (GWAS) was performed on the phenotypes obtained from the 270 *A. thaliana* natural accessions that survived and grew on the SCS. Phenotypes included leaf mineral concentrations of 11 elements (Fe, Mg, Ca, K, Na, S, Mn, B, P, Zn and Mo) of three 55-days old plants. Cu and Ni were below the level of detection and could not be quantified. All the phenotypes are detailed in Table S1 and Figure S4.

GWA mapping was performed in GEMMA (version 0.98) (Zhou & Stephens, 2012) with a univariate linear mixed model and the minor allele frequency cut-off set at 0.1. GWAS was run with the imputed 1 348 843 SNP set (*Arabidopsis\_2029\_Maf001\_Filter80*) (Arouisse et al., 2020). A kinship matrix was constructed in GEMMA to correct for population structure and individual relatedness. The Benjamini & Hochberg threshold (BH) was implemented using the formula  $(i/m) Q$ , where:  $i$  = the individual  $P$ -value's rank,  $m$  = total number of tests,  $Q$  = the false discovery rate set at 25%. This corresponded to a BH threshold of 6.42. SNPs with score above BH correction and  $m.a.f > 0.1$  were selected and the linkage disequilibrium (LD) region associated with the highest score SNP was explored to identify candidate genes for the causal allelic variant. All genes associated with the significant SNPs and their SNPs in strong LD ( $r^2 > 0.8$ ) were explored (Table S3). Genes were annotated according to TAIR 10 (Araport11).

### Candidate genes validation

Seeds from 9 selected *A. thaliana* accessions, Col-0 and 17T-DNA insertion lines were obtained from the *A. thaliana* Stock Centre (NASC, Nottingham, United Kingdom). Each ExtP group (displaying contrasted phenotypes for leaf Na and Fe concentration and bearing contrasted alleles at the candidate SNPs) was a pool of 3 accessions. Figure S1 details the workflow and the *A. thaliana* natural accessions and mutants used in each experiment. *A. thaliana* natural accessions were classified as "High Leaf Na" (HLNa), "Low Leaf Na Lead" (LLNa), "High Leaf Fe Lead" (HLFe) or "Low Leaf Fe" (LLFe) based on their leaf Na and Fe concentrations on SCS. In all soil, hydroponic and plate experiments, seeds were surface sterilized and stratified as described above to synchronize germination.

### Soil pot culture

Seeds were sown into the same soil type used for the HapMap screening. Each tray contained 24 individuals in a random block design with a total of six individuals per accession and soil type. Plants were allowed to germinate and grow at 10 h light/14 h dark at 25°C to 20°C day/night temperature, 150  $\mu\text{mol m}^{-2} \text{sec}^{-1}$  and 40% humidity. Trays were bottom watered twice weekly with deionized water. Rosette diameter (RD) from the third week to the end of the experiment was measured from aerial pictures. Two leaves from 55-day-old plants were collected from up to six plants per accession and soil type.

### Hydroponic culture

Seeds were germinated in a mix of sand and perlite (3:1) and 10-day old seedlings were transferred to individual round hydroponic containers (100 ml) filled with 0.5-strength Hoagland solution (pH 5.7) and no NaCl or NaHCO<sub>3</sub> added (control) or containing 40 mM NaCl + 10 mM NaHCO<sub>3</sub>, set at pH 8.3 (treatment). Plants germinated and grew at 10 h light/14 h dark, 25°C to 20°C day/night temperature, 150 μmol cm<sup>-2</sup> sec<sup>-1</sup> PAR and 40% humidity. The hydroponic solution was changed every 3 days to maintain a relatively constant concentration of nutrients in the solution and treatment concentrations were increased two times - 20 mM NaCl + 5 mM NaHCO<sub>3</sub> at pH 8.3, and 30 mM NaCl + 15 mM NaHCO<sub>3</sub> at pH 8.3 - until reaching the final concentration of 40 mM NaCl + 10 mM NaHCO<sub>3</sub>, at pH 8.3, when plants were 21 days old. Plants remained at these conditions for two more weeks. 35-days old plants were harvested and root length, rosette diameter and total fresh weight (biomass) of the six individuals per accession and per treatment were measured. Roots and leaves from the six plants per accession were stored for ionome and gene expression analysis.

### Plate culture

For germination assays, 10 seeds from each accession were sown in plates in a laminar air flow cabinet with sterile material. Plates were made for two treatments: control (½ MS at pH 5.9) and bicarbonate (½ MS at pH 8.3 and 10 mM NaHCO<sub>3</sub>). All plates contained Phyto-agar 0.6% (Duchefa, Haarlem, The Netherlands), and solutions were buffered with MES (2-(N-morpholino) ethanesulfonic acid) and BTP (Bis-Tris Propane) depending on final pH. Plates with seeds were kept at 4°C for synchronizing germination. After 7 days under stratification treatment, plates were moved to a growth chamber (12 h light/12 h dark, 150 μmol m<sup>-2</sup> sec<sup>-1</sup>, 40% humidity and 25°C). Germination was checked every day for 2 weeks and treatment effects were recorded as (% Alk-Sal germination / % C-germination). Seeds of *ninja* and SALK\_069095.55.25 mutant were not available at the time of plate experimental setup and were not assessed for germination.

### Gene expression analyses

Total RNA of about 100 mg of plant leaf material was extracted using the MaxwellRSC plant RNA kit (Promega Corporation, Madison, WI, USA) following the manufacturer's instructions. Two micrograms of total RNA were used as a template to synthesize first-strand cDNA with the iScriptTM cDNA Synthesis Kit (Bio-Rad, Foster City, CA, USA). The cDNA was used as a template for Reverse-Transcriptase quantitative real-time PCR (RT-qPCR) using iTaqTM Universal SYBR Green Supermix (Bio-Rad). Real-time detection of fluorescence emission was performed on a CFX384 Real-Time System (Bio-Rad), and plates were edited using the CFX manager version 3.1 software. Primers used for pinpointed candidate genes transcript quantification - *PGP10*, *NINJA*, *YUC8*, *ALA3* - in selected natural accessions showing contrasted phenotypes are detailed in Table S2. Relative quantifications were performed for all genes with the *Actin2* gene (AT3G18780) used as an internal reference. For each sample, the average value from triplicate RT-qPCRs was used to estimate transcript abundance. Four samples per line were used. The mean Ct values were normalized against *Actin2* and dCt values were calculated as (dCtGene/dCtActin2). The data are expressed as means ± SE relative to the Col-0 value (defined as 1).

### Statistical analyses

All the statistical analyses were conducted using JMP SAS software (SAS Institute, Cary, NC, USA). No data normalization was applied. To compensate for variation between and within trays, outlier samples that were 4.5 times higher than the interquartile range across all trays per each element were excluded from the descriptive analysis. This threshold was chosen over the more standard 1.5 times threshold according to Campos et al. (2021), to include accessions with an extreme phenotype.

In all soil and hydroponic cultures, mean-standardized values ( $-1 < \text{value} < 1$ ) of elemental contents of soil and leaf material were used to represent the radar plots and compare between soil types, treatments or accessions, and One-way ANOVA was used to test for significant differences ( $P < 0.05$ ) between means of phenotypic responses, gene expression, and between means of elemental contents of soil and leaf material. To perform multiple comparisons of group means we used Tukey's HSD and to compare elemental profiles of each mutant with Col-0 (WT) we used Dunnett's test.

To investigate changes in root length (RL), rosette diameter (RD) and fresh weight (Biomass) in the hydroponic experiment, where a control treatment was available, the phenotypic responses to saline-carbonated conditions were quantified and compared to the respective control conditions [relative measurements: mean (XTreatment) = mean(XControl)].

Statistical data analyses are specified in Datasets S1–S5.

### ACCESSION NUMBERS

Accessions numbers are listed in Supporting Information Table S1.

### AUTHORS CONTRIBUTION

MJ-A and LP-M performed the lab experiments. MJ-A, RB and SB performed data analysis. MJ-A, LP-M, ML and CP conceived the study. All authors contributed to the writing of the manuscript.

### ACKNOWLEDGEMENTS

Special thanks to Rosa Padilla to process ICP field and soil samples. The authors are grateful to the Nottingham Arabidopsis Stock Centre for the Arabidopsis seeds, to Dr. Ritter and Dr. Goossens, from the Specialized Metabolism Research Group at VIB-Ugent Center for Plant Systems Biology (Ghent University) for *ninja* knockout mutant seeds, and to Dr. Terés and Dr. Salt for sharing ionic data for comparative purposes. This research was supported by the Spanish Ministry of Science and Innovation (MICINN) (PID 2019 104000 RB I00).

### CONFLICT OF INTEREST

The authors declare no conflicts of interest.

### SUPPORTING INFORMATION

Additional Supporting Information may be found in the online version of this article.

**Figure S1.** Flowchart of the experimental procedure. Different color boxes define plant material used at each experimental stage: Turquoise: HapMap cohort accessions; Purple: Col-0 (Wild-Type) and T-DNA insertion mutant lines.



**Figure S2.** Nutrient ratios in leaves of the *A. thaliana* accessions used in the study.

**Figure S3.** Correlogram (a), clustered heatmap (b) and scatter plot matrix (c) of leaf element concentrations across the studied *A. thaliana* accessions.

**Figure S4.** Genome wide association studies (GWAS) for leaf B, Ca, K, Mg, Mn, P, S, Zn ionome traits of HapMap accessions grown on SCS.

**Figure S5.** SNP specificity of the identified candidate genes.

**Table S1.** Leaf mineral nutrition, growth classification and native soil characterization of the natural accessions collection used.

**Table S2.** Primer set used for RT-qPCR expression analyses.

**Table S3.** List for significant associations and corresponding QTLs detected by GWA mapping of Leaf Na and Fe concentration of plants grown on saline-calcareous study soil (SCS).

**Table S4.** List for candidate gene T-DNA insertion mutant lines for leaf Na (LNa) and leaf Fe (LFe) phenotyping.

**Table S5.** List for natural populations displaying extreme phenotypes and contrasted alleles selected for growth, ionome and candidate gene leaf and root expression analyses (ExtP accessions).

**Table S6.** SNP polymorphisms surrounding the *YUC8*, *NINJA* and *ALA3* locus in LD with the significant GWAS SNP.

**Table S7.** Potentially causal SNPs for allelic variation of the identified candidate genes. Table shows Phenotype of SNP association (Leaf Na: LNa; leaf Fe: LFe), Gene, Gene Id, splice variant when described, Position, variant length (bp), variant description (base substitution); Reference (Ref) and Alternative (Alt) allele versions and type of variant according to the affected region.

## REFERENCES

- Akhtar, M., Yousaf, S., Sarwar, N. & Hussain, S. (2019) Zinc biofortification of cereals—role of phosphorus and other impediments in alkaline calcareous soils. *Environmental Geochemistry and Health*, **41**(5), 2365–2379. Available from: <https://doi.org/10.1007/s10653-019-00279-6>
- Alloway, B.J. (2013) Molybdenum. In: *Heavy metals in soils*. Dordrecht: Springer, pp. 527–534.
- Arouisse, B., Korte, A., van Eeuwijk, F. & Kruijer, W. (2020) Imputation of 3 million SNPs in the Arabidopsis regional mapping population. *The Plant Journal*, **102**(4), 872–882. Available from: <https://doi.org/10.1111/tpj.14659>
- Assefa, T., Zhang, J., Chowda-Reddy, R.V., Moran Lauter, A.N., Singh, A., O'Rourke, J.A. et al. (2020) Deconstructing the genetic architecture of iron deficiency chlorosis in soybean using genome-wide approaches. *BMC Plant Biology*, **20**(1), 1–13. Available from: <https://doi.org/10.1186/s12870-020-2237-5>
- Atwell, S., Huang, Y.S., Vilhjálmsson, B.J., Willems, G., Horton, M., Li, Y. et al. (2010) Genome-wide association study of 107 phenotypes in *Arabidopsis thaliana* inbred lines. *Nature*, **465**(7298), 627–631. Available from: <https://doi.org/10.1038/nature08800>
- Babuín, M.F., Campestre, M.P., Rocco, R., Bordenave, C.D., Escaray, F.J., Antonelli, C. et al. (2014) Response to long-term NaHCO<sub>3</sub>-derived alkalinity in model Lotus japonicus ecotypes Gifu B-129 and Miyakojima MG-20: transcriptomic profiling and physiological characterization. *PLoS One*, **9**(5), e97106. Available from: <https://doi.org/10.1371/journal.pone.0097106>
- Bacha, H., Ródenas, R., López-Gómez, E., García-Legaz, M.F., Nieves-Cordones, M., Rivero, R.M. et al. (2015) High Ca<sup>2+</sup> reverts the repression of high-affinity K<sup>+</sup> uptake produced by Na<sup>+</sup> in solanum lycopersicum L.(var. microtom) plants. *Journal of Plant Physiology*, **180**, 72–79. Available from: <https://doi.org/10.1016/j.jplph.2015.03.014>
- Bahmani, K., Sadat-Noori, S.A., Izadi, A. & Akbari, A. (2015) Molecular mechanisms of plant salinity tolerance: a review. *Australian Journal of Crop Science*, **9**, 321–336. Available from: <https://doi.org/10.3316/inform.132428657147758>
- Bai, J., Yan, W., Wang, Y., Yin, Q., Liu, J., Wight, C. et al. (2018) Screening oat genotypes for tolerance to salinity and alkalinity. *Frontiers in Plant Science*, **9**, 1302. Available from: <https://doi.org/10.3389/fpls.2018.01302>
- Baxter, I., Brazelton, J.N., Yu, D., Huang, Y.S., Lahner, B., Yakubova, E. et al. (2010) A coastal cline in sodium accumulation in *Arabidopsis thaliana* is driven by natural variation of the sodium transporter AtHKT1; 1. *PLoS Genetics*, **6**(11), e1001193. Available from: <https://doi.org/10.1371/journal.pgen.1001193>
- Baxter, I. & Dilkes, B.P. (2012) Elemental profiles reflect plant adaptations to the environment. *Science*, **336**(6089), 1661–1663. Available from: <https://doi.org/10.1126/science.1219992>
- Baxter, I., Muthukumar, B., Park, H.C., Buchner, P., Lahner, B., Danku, J. et al. (2008) Variation in molybdenum content across broadly distributed populations of *Arabidopsis thaliana* is controlled by a mitochondrial molybdenum transporter (MOT1). *PLoS Genetics*, **4**(2), e1000004. Available from: <https://doi.org/10.1371/journal.pgen.1000004>
- Bazakos, C., Hanemian, M., Trontin, C., Jimenez-Gomez, J.M. & Loudet, O. (2017) New strategies and tools in quantitative genetics: how to go from the phenotype to the genotype. *Annual Review of Plant Biology*, **68**, 435–455. Available from: <https://doi.org/10.1146/annurev-arplant-042916-040820>
- Ben Abdallah, H., Mai, H.J., Álvarez-Fernández, A., Abadía, J. & Bauer, P. (2017) Natural variation reveals contrasting abilities to cope with alkaline and saline soil among different *Medicago truncatula* genotypes. *Plant and Soil*, **418**(1), 45–60. Available from: <https://doi.org/10.1007/s11104-017-3379-6>
- Bian, C., Guo, X., Zhang, Y., Wang, L., Xu, T., DeLong, A. et al. (2020) Protein phosphatase 2A promotes stomatal development by stabilizing SPEECHLESS in Arabidopsis. *Proceedings of the National Academy of Sciences of the United States of America*, **117**(23), 13127–13137. Available from: <https://doi.org/10.1073/pnas.1912075117>
- Bittner, F. (2014) Molybdenum metabolism in plants and crosstalk to iron. *Frontiers in Plant Science*, **5**, 28. Available from: <https://doi.org/10.3389/fpls.2014.00028>
- Busoms, S., Paajanen, P., Marburger, S., Bray, S., Huang, X.Y., Poschenrieder, C. et al. (2018) Fluctuating selection on migrant adaptive sodium transporter alleles in coastal *Arabidopsis thaliana*. *Proceedings of the National Academy of Sciences of the United States of America*, **115**(52), E12443–E12452. Available from: <https://doi.org/10.1073/pnas.1816964115>
- Cackett, L., Cannistraci, C.V., Meier, S., Ferrandi, P., Pěncík, A., Gehring, C. et al. (2022) Salt-specific gene expression reveals elevated auxin levels in *Arabidopsis thaliana* plants grown under saline conditions. *Frontiers in Plant Science*, **13**, 804716. Available from: <https://doi.org/10.3389/fpls.2022.804716>
- Cakmak, I. (2000) Tansley review No. 111 possible roles of zinc in protecting plant cells from damage by reactive oxygen species. *The New Phytologist*, **146**(2), 185–205. Available from: <https://doi.org/10.1046/j.1469-8137.2000.00630.x>
- Campos, A.C.A.L., van Dijk, W., Ramakrishna, P., Giles, T.C., Korte, P., Douglas, A. et al. (2021) 1,135 ionomes reveal the global pattern of leaf and seed mineral nutrient and trace element diversity in *Arabidopsis thaliana*. *The Plant Journal*, **106**, 536–554. Available from: <https://doi.org/10.1111/tpj.15177>
- Cao, Y., Zhang, M., Liang, X., Li, F., Shi, Y., Yang, X. et al. (2020) Natural variation of an EF-hand Ca<sup>2+</sup>-binding-protein coding gene confers saline-alkaline tolerance in maize. *Nature Communications*, **11**(1), 1–14. Available from: <https://doi.org/10.1038/s41467-019-14027-y>
- Celletti, S., Pii, Y., Valentinuzzi, F., Tiziani, R., Fontanella, M.C., Beone, G.M. et al. (2020) Physiological responses to Fe deficiency in split-root tomato plants: possible roles of auxin and ethylene? *Agronomy*, **10**(7), 1000. Available from: <https://doi.org/10.3390/agronomy10071000>
- Chaurasia, S., Singh, A.K., Kumar, A., Songachan, L.S., Yadav, M.C., Kumar, S. et al. (2021) Genome-wide association mapping reveals key genomic regions for physiological and yield-related traits under salinity stress in wheat (*Triticum aestivum* L.). *Genomics*, **113**(5), 3198–3215. Available from: <https://doi.org/10.1016/j.ygeno.2021.07.014>
- Couturier, J., Ströher, E., Albetel, A.N., Roret, T., Muthuramalingam, M., Tarrago, L. et al. (2011) Arabidopsis chloroplastic glutaredoxin C5 as a model to explore molecular determinants for iron-sulfur cluster binding into glutaredoxins. *Journal of Biological Chemistry*, **286**(31), 27515–27527. Available from: <https://doi.org/10.1074/jbc.M111.228726>
- Davila Olivas, N.H., Frago, E., Thoen, M., Kloth, K.J., Becker, F., van Loon, J. et al. (2017) Natural variation in life history strategy of *Arabidopsis thaliana* determines stress responses to drought and insects of different

- feeding guilds. *Molecular Ecology*, **26**(11), 2959–2977. Available from: <https://doi.org/10.1111/mec.14100>
- de Santiago-Martín, A., Valverde-Asenjo, I., Quintana, J.R., González, C. & Lafuente, A.L. (2013) Soil properties affecting metal extractability pattern in periurban calcareous agricultural soils in the Mediterranean area. *International Journal of Environmental Research*, **7**(4), 831–840.
- Deinlein, U., Stephan, A.B., Horie, T., Luo, W., Xu, G. & Schroeder, J.I. (2014) Plant salt tolerance mechanisms. *Trends in Plant Science*, **19**(6), 371–379. Available from: <https://doi.org/10.1016/j.tplants.2014.02.001>
- Do, T.D., Vuong, T.D., Dunn, D., Clubb, M., Valliyodan, B., Patil, G. *et al.* (2019) Identification of new loci for salt tolerance in soybean by high-resolution genome-wide association mapping. *BMC Genomics*, **20**(1), 1–16. Available from: <https://doi.org/10.1186/s12864-019-5662-9>
- Edwards, N.C., Hing, Z.A., Perry, A., Blaisdell, A., Kopelman, D.B., Fathke, R. *et al.* (2012) Characterization of coding synonymous and non-synonymous variants in ADAMTS13 using ex vivo and in silico approaches. *PLoS One*, **7**(6), e38864. Available from: <https://doi.org/10.1371/journal.pone.0038864>
- Erice, G., Ruiz-Lozano, J.M., Zamarreño, Á.M., García-Mina, J.M. & Aroca, R. (2017) Transcriptomic analysis reveals the importance of JA-Ile turnover in the response of Arabidopsis plants to plant growth promoting rhizobacteria and salinity. *Environmental and Experimental Botany*, **143**, 10–19. Available from: <https://doi.org/10.1016/j.envexpbot.2017.08.006>
- Eroglu, S., Meier, B., von Wirén, N. & Peiter, E. (2016) The vacuolar manganese transporter MTP8 determines tolerance to iron deficiency-induced chlorosis in Arabidopsis. *Plant Physiology*, **170**(2), 1030–1045. Available from: <https://doi.org/10.1104/pp.15.01194>
- Fan, G.A.O., Qiang, H.U.A.N.G., Xiaoyi, S.U.N. & Zhenglong, Y.A.N. (2011) Study on dynamic changes of the soil salinization in the upper stream of the Tarim River based on RS and GIS. *Procedia Environmental Sciences*, **11**, 1135–1141. Available from: <https://doi.org/10.1016/j.proenv.2011.12.171>
- Fan, Y., Zhou, G., Shabala, S., Chen, Z.H., Cai, S., Li, C. *et al.* (2016) Genome-wide association study reveals a new QTL for salinity tolerance in barley (*Hordeum vulgare* L.). *Frontiers in Plant Science*, **7**, 946. Available from: <https://doi.org/10.3389/fpls.2016.00946>
- Fang, S., Hou, X. & Liang, X. (2021) Response mechanisms of plants under saline-alkaline stress. *Frontiers in Plant Science*, **12**, 667458. Available from: <https://doi.org/10.3389/fpls.2021.667458>
- FAO. (1973) Report of the FAO/UNDP regional seminar on reclamations and management of calcareous soils FAO Soils Bulletin 21, Calcareous soils. FAO-UN Rome. ISBN 92-5-100276-2. <https://www.fao.org/3/x5868e/x5868e00.htm>
- Greenbaum, J. & Deng, H.W. (2017) A statistical approach to fine mapping for the identification of potential causal variants related to bone mineral density. *Journal of Bone and Mineral Research*, **32**(8), 1651–1658. Available from: <https://doi.org/10.1002/jbmr.3154>
- Grodecká, L., Buratti, E. & Freiberger, T. (2017) Mutations of pre-mRNA splicing regulatory elements: are predictions moving forward to clinical diagnostics? *International Journal of Molecular Sciences*, **18**(8), 1668. Available from: <https://doi.org/10.3390/ijms18081668>
- Hantzis, L.J., Kroh, G.E., Jahn, C.E., Cantrell, M., Peers, G., Pilon, M. *et al.* (2018) A program for iron economy during deficiency targets specific Fe responses. *Plant Physiology*, **176**(1), 596–610. Available from: <https://doi.org/10.1104/pp.17.01497>
- Haro, R., Bañuelos, M.A., Senn, M.E., Barrero-Gil, J. & Rodríguez-Navarro, A. (2005) HKT1 mediates sodium uniprot in roots. Pitfalls in the expression of HKT1 in yeast. *Plant Physiology*, **139**(3), 1495–1506. Available from: <https://doi.org/10.1104/pp.105.067553>
- Hazzouri, K.M., Khraiwesh, B., Amiri, K.M., Pauli, D., Blake, T., Shahid, M. *et al.* (2018) Mapping of HKT1; 5 gene in barley using GWAS approach and its implication in salt tolerance mechanism. *Frontiers in Plant Science*, **9**, 156. Available from: <https://doi.org/10.3389/fpls.2018.00156>
- He, Y., Wu, D., Wei, D., Fu, Y., Cui, Y., Dong, H. *et al.* (2017) GWAS, QTL mapping and gene expression analyses in Brassica napus reveal genetic control of branching morphogenesis. *Scientific Reports*, **7**(1), 1–9. Available from: <https://doi.org/10.1038/s41598-017-15976-4>
- Hentrich, M., Böttcher, C., Dücking, P., Cheng, Y., Zhao, Y., Berkowitz, O. *et al.* (2013) The jasmonic acid signaling pathway is linked to auxin homeostasis through the modulation of YUCCA 8 and YUCCA 9 gene expression. *The Plant Journal*, **74**(4), 626–637. Available from: <https://doi.org/10.1111/tpj.12152>
- Horton, M., Hancock, A.M., Huang, Y.S., Toomajian, C., Atwell, S., Anton, A. *et al.* (2012) Genome-wide pattern of genetic variation in worldwide *Arabidopsis thaliana* accessions from the RegMap panel. *Nature Genetics*, **44**(2), 212–216. Available from: <https://doi.org/10.1038/ng.1042>
- Hsieh, E.J. & Waters, B.M. (2016) Alkaline stress and iron deficiency regulate iron uptake and riboflavin synthesis gene expression differently in root and leaf tissue: implications for iron deficiency chlorosis. *Journal of Experimental Botany*, **67**(19), 5671–5685. Available from: <https://doi.org/10.1093/jxb/erw328>
- Hu, R., Zhu, Y., Shen, G. & Zhang, H. (2017) Overexpression of the PP2A-C5 gene confers increased salt tolerance in Arabidopsis thaliana. *Plant Signaling & Behavior*, **12**(2), e1276687. Available from: <https://doi.org/10.1080/15592324.2016.1276687>
- Hu, X., Wang, D., Ren, S., Feng, S., Zhang, H., Zhang, J. *et al.* (2022) Inhibition of root growth by alkaline salts due to disturbed ion transport and accumulation in *Leymus chinensis*. *Environmental and Experimental Botany*, **104907**, 104907. Available from: <https://doi.org/10.1016/j.envexpbot.2022.104907>
- Huang, R.D. (2018) Research progress on plant tolerance to soil salinity and alkalinity in sorghum. *Journal of Integrative Agriculture*, **17**(4), 739–746. Available from: [https://doi.org/10.1016/S2095-3119\(17\)61728-3](https://doi.org/10.1016/S2095-3119(17)61728-3)
- Iglesias, M.J., Terrile, M.C., Windels, D., Lombardo, M.C., Bartoli, C.G., Vazquez, F. *et al.* (2014) MiR393 regulation of auxin signaling and redox-related components during acclimation to salinity in Arabidopsis. *PLoS One*, **9**(9), e107678. Available from: <https://doi.org/10.1371/journal.pone.0107678>
- Ismail, A., Seo, M., Takebayashi, Y., Kamiya, Y., Eiche, E. & Nick, P. (2014) Salt adaptation requires efficient fine-tuning of jasmonate signalling. *Protoplasma*, **251**(4), 881–898. Available from: <https://doi.org/10.1007/s00709-013-0591-y>
- Jin, T., Sun, Y., Shan, Z., He, J., Wang, N., Gai, J. *et al.* (2021) Natural variation in the promoter of GsERD15B affects salt tolerance in soybean. *Plant Biotechnology Journal*, **19**(6), 1155–1169. Available from: <https://doi.org/10.1111/pbi.13536>
- Jobbágy, E.G., Tóth, T., Nosetto, M.D. & Earman, S. (2017) On the fundamental causes of high environmental alkalinity (pH ≥ 9): an assessment of its drivers and global distribution. *Land Degradation & Development*, **28**(7), 1973–1981. Available from: <https://doi.org/10.1002/ldr.2718>
- Julkowska, M.M., Hoefsloot, H.C., Mol, S., Feron, R., de Boer, G.J., Haring, M.A. *et al.* (2014) Capturing Arabidopsis root architecture dynamics with ROOT-FIT reveals diversity in responses to salinity. *Plant Physiology*, **166**(3), 1387–1402. Available from: <https://doi.org/10.1104/pp.114.248963>
- Julkowska, M.M., Koevoets, I.T., Mol, S., Hoefsloot, H., Feron, R., Tester, M.A. *et al.* (2017) Genetic components of root architecture remodeling in response to salt stress. *The Plant Cell*, **29**(12), 3198–3213. Available from: <https://doi.org/10.1105/tpc.16.00680>
- Katori, T., Ikeda, A., Iuchi, S., Kobayashi, M., Shinozaki, K., Maehashi, K. *et al.* (2010) Dissecting the genetic control of natural variation in salt tolerance of *Arabidopsis thaliana* accessions. *Journal of Experimental Botany*, **61**, 1125–1138. Available from: <https://doi.org/10.1093/jxb/erp376>
- Kawa, D., Julkowska, M.M., Sommerfeld, H.M., Ter Horst, A., Haring, M.A. & Testerink, C. (2016) Phosphate-dependent root system architecture responses to salt stress. *Plant Physiology*, **172**(2), 690–706. Available from: <https://doi.org/10.1104/pp.16.00712>
- Knight, H., Trewavas, A.J. & Knight, M.R. (1997) Calcium signalling in *Arabidopsis thaliana* responding to drought and salinity. *The Plant Journal*, **12**(5), 1067–1078. Available from: <https://doi.org/10.1046/j.1365-313X.1997.12051067.x>
- Korte, A. & Farlow, A. (2013) The advantages and limitations of trait analysis with GWAS: a review. *Plant Methods*, **9**(1), 1–9. Available from: <https://doi.org/10.1186/1746-4811-9-29>
- Kumar, V., Singh, A., Mithra, S.A., Krishnamurthy, S.L., Parida, S.K., Jain, S. *et al.* (2015) Genome-wide association mapping of salinity tolerance in rice (*Oryza sativa*). *DNA Research*, **22**(2), 133–145. Available from: <https://doi.org/10.1093/dnares/dsu046>
- Laurie, S., Feeney, K.A., Maathuis, F.J., Heard, P.J., Brown, S.J. & Leigh, R.A. (2002) A role for HKT1 in sodium uptake by wheat roots. *The Plant Journal*, **32**(2), 139–149. Available from: <https://doi.org/10.1046/j.1365-313X.2002.01410.x>

- Li, B. (2020) Identification of genes conferring plant salt tolerance using GWAS: current success and perspectives. *Plant and Cell Physiology*, **61** (8), 1419–1426. Available from: <https://doi.org/10.1093/pcp/pcaa073>
- Li, J., Jia, Y., Dong, R., Huang, R., Liu, P., Li, X. *et al.* (2019) Advances in the mechanisms of plant tolerance to manganese toxicity. *International Journal of Molecular Sciences*, **20**(20), 5096. Available from: <https://doi.org/10.3390/ijms20205096>
- Li, Q., Yang, A. & Zhang, W.H. (2016) Efficient acquisition of iron confers greater tolerance to saline-alkaline stress in rice (*Oryza sativa* L.). *Journal of Experimental Botany*, **67**, erw407. Available from: <https://doi.org/10.1093/jxb/erw407>
- Liu, S., Zhong, H., Meng, X., Sun, T., Li, Y., Pinson, S.R. *et al.* (2020) Genome-wide association studies of ionic and agronomic traits in USDA mini core collection of rice and comparative analyses of different mapping methods. *BMC Plant Biology*, **20**(1), 1–18. Available from: <https://doi.org/10.1186/s12870-020-02603-0>
- Liu, Y., Chen, X., Xue, S., Quan, T., Cui, D., Han, L. *et al.* (2021) SET DOMAIN GROUP 721 protein functions in saline-alkaline stress tolerance in the model rice variety Kitaake. *Plant Biotechnology Journal*, **19**(12), 2576–2588. Available from: <https://doi.org/10.1111/pbi.13683>
- Liu, Y., Wang, L., Deng, M., Li, Z., Lu, Y., Wang, J. *et al.* (2015) Genome-wide association study of phosphorus-deficiency-tolerance traits in *Aegilops tauschii*. *Theoretical and Applied Genetics*, **128**(11), 2203–2212. Available from: <https://doi.org/10.1007/s00122-015-2578-x>
- López-Marqués, R.L., Davis, J.A., Harper, J.F. & Palmgren, M. (2021) Dynamic membranes: the multiple roles of P4 and P5 ATPases. *Plant Physiology*, **185**(3), 619–631. Available from: <https://doi.org/10.1093/plphys/kiab065>
- Mamidi, S., Lee, R.K., Goos, J.R. & McClean, P.E. (2014) Genome-wide association studies identifies seven major regions responsible for iron deficiency chlorosis in soybean (*Glycine max*). *PLoS One*, **9**(9), e107469. Available from: <https://doi.org/10.1371/journal.pone.0107469>
- Maris, A., Suslov, D., Fry, S.C., Verbelen, J.P. & Vissenberg, K. (2009) Enzymic characterization of two recombinant xyloglucan endotransglucosylase/hydrolase (XTH) proteins of *Arabidopsis* and their effect on root growth and cell wall extension. *Journal of Experimental Botany*, **60**(13), 3959–3972. Available from: <https://doi.org/10.1093/jxb/erp229>
- Máthé, C., Garda, T., Freytag, C. & M-Hamvas, M. (2019) The role of serine-threonine protein phosphatase PP2A in plant oxidative stress signaling—facts and hypotheses. *International Journal of Molecular Sciences*, **20** (12), 3028. Available from: <https://doi.org/10.3390/ijms20123028>
- McDowell, S.C., Lopez-Marques, R.L., Poulsen, L.R., Palmgren, M.G. & Harper, J.F. (2013) Loss of the *Arabidopsis thaliana* P4-ATPase ALA3 reduces adaptability to temperature stresses and impairs vegetative, pollen, and ovule development. *PLoS One*, **8**(5), e62577. Available from: <https://doi.org/10.1371/journal.pone.0062577>
- Mendoza-Cózatl, D.G., Gokul, A., Carelse, M.F., Jobe, T.O., Long, T.A. & Keyster, M. (2019) Keep talking: crosstalk between iron and sulfur networks fine-tunes growth and development to promote survival under iron limitation. *Journal of Experimental Botany*, **70**(16), 4197–4210. Available from: <https://doi.org/10.1093/jxb/erz290>
- Mengel, K. & Kirkby, E.A. (2001) *Principles of plant nutrition*, 5th edition. Dordrecht, Netherlands: Kluwer Academic Publication.
- Miller, C.N. & Busch, W. (2021) Using natural variation to understand plant responses to iron availability. *Journal of Experimental Botany*, **72**(6), 2154–2164. Available from: <https://doi.org/10.1093/jxb/erab012>
- Milner, M.J., Seamon, J., Craft, E. & Kochian, L.V. (2013) Transport properties of members of the ZIP family in plants and their role in Zn and Mn homeostasis. *Journal of Experimental Botany*, **64**(1), 369–381. Available from: <https://doi.org/10.1093/jxb/ers315>
- Møller, I.S., Gilliam, M., Jha, D., Mayo, G.M., Roy, S.J., Coates, J.C. *et al.* (2009) Shoot Na<sup>+</sup> exclusion and increased salinity tolerance engineered by cell type-specific alteration of Na<sup>+</sup> transport in *Arabidopsis*. *The Plant Cell*, **21**(7), 2163–2178. Available from: <https://doi.org/10.1105/tpc.108.064568>
- Mwando, E., Han, Y., Angessa, T.T., Zhou, G., Hill, C.B., Zhang, X.Q. *et al.* (2020) Genome-wide association study of salinity tolerance during germination in barley (*Hordeum vulgare* L.). *Frontiers in Plant Science*, **11**, 118. Available from: <https://doi.org/10.3389/fpls.2020.00118>
- Nayyeripasand, L., Garoosi, G.A. & AhmadiKah, A. (2021) Genome-wide association study (GWAS) to identify salt-tolerance QTLs carrying novel candidate genes in rice during early vegetative stage. *Rice*, **14**(1), 1–21. Available from: <https://doi.org/10.1186/s12284-020-00433-0>
- Ogura, T. & Busch, W. (2015) From phenotypes to causal sequences: using genome wide association studies to dissect the sequence basis for variation of plant development. *Current Opinion in Plant Biology*, **23**, 98–108. Available from: <https://doi.org/10.1016/j.pbi.2014.11.008>
- Ostaszewska, M., Juszczak, I.M., Kołodziejek, I. & Rychter, A.M. (2014) Long-term Sulphur starvation of *Arabidopsis thaliana* modifies mitochondrial ultrastructure and activity and changes tissue energy and redox status. *Journal of Plant Physiology*, **171**(7), 549–558. Available from: <https://doi.org/10.1016/j.jplph.2013.12.013>
- Panagos, P., Meusburger, K., Alewell, C. & Montanarella, L. (2012) Soil erodibility estimation using LUCAS point survey data of Europe. *Environmental Modelling & Software*, **30**, 143–145. Available from: <https://doi.org/10.1016/j.envsoft.2011.11.002>
- Pauwels, L., Barbero, G.F., Geerinck, J., Tillemans, S., Grunewald, W., Pérez, A.C. *et al.* (2010) NINJA connects the co-repressor TOPLESS to jasmonate signalling. *Nature*, **464**(7289), 788–791. Available from: <https://doi.org/10.1038/nature08854>
- Pérez-Martin, L. (2020) Physiological, molecular and genetic mechanisms of adaptation to alkaline and saline soils in *Arabidopsis thaliana* populations. Doctoral dissertation, Ph. D. Thesis Universitat Autònoma de Barcelona. <https://ddd.uab.cat/record/256996>
- Pérez-Martin, L., Busoms, S., Almira, M.J., Azagury, N., Terés, J., Tolrà, R. *et al.* (2022) Evolution of salt tolerance in *Arabidopsis thaliana* on siliceous soils does not confer tolerance to saline calcareous soils. *Plant and Soil*, **1–21**, 455–475. Available from: <https://doi.org/10.1007/s11104-022-05439-9>
- Pineau, C., Loubet, S., Lefoulon, C., Chaliès, C., Fizames, C., Lacombe, B. *et al.* (2012) Natural variation at the FRD3 MATE transporter locus reveals cross-talk between Fe homeostasis and Zn tolerance in *Arabidopsis thaliana*. *PLoS Genetics*, **8**(12), e1003120. Available from: <https://doi.org/10.1371/journal.pgen.1003120>
- Poulsen, L.R., López-Marqués, R.L., McDowell, S.C., Okkeri, J., Licht, D., Schulz, A. *et al.* (2008) The *Arabidopsis* P4-ATPase ALA3 localizes to the Golgi and requires a  $\beta$ -subunit to function in lipid translocation and secretory vesicle formation. *The Plant Cell*, **20**(3), 658–676. Available from: <https://doi.org/10.1105/tpc.107.054767>
- Poulsen, L.R., López-Marqués, R.L., McDowell, S.C., Okkeri, J., Licht, D., Schulz, A. *et al.* (2008) The *Arabidopsis* P4-ATPase ALA3 localizes to the Golgi and requires a  $\beta$ -subunit to function in lipid translocation and secretory vesicle formation. *Plant Cell*, **20**, 658–676. Available from: <https://doi.org/10.1105/tpc.107.054767>
- Qiao, Y., Jiang, W., Lee, J., Park, B., Choi, M.S., Piao, R. *et al.* (2010) SPL28 encodes a clathrin-associated adaptor protein complex 1, medium subunit  $\mu$ 1 (AP1M1) and is responsible for spotted leaf and early senescence in rice (*Oryza sativa*). *New Phytologist*, **185**(1), 258–274. Available from: <https://doi.org/10.1111/j.1469-8137.2009.03047.x>
- Qin, H., Zhang, Z., Wang, J., Chen, X., Wei, P. & Huang, R. (2017) The activation of OSEIL1 on YUC8 transcription and auxin biosynthesis is required for ethylene-inhibited root elongation in rice early seedling development. *PLoS Genetics*, **13**(8), e1006955. Available from: <https://doi.org/10.1371/journal.pgen.1006955>
- Rabhi, M., Barhoumi, Z., Ksouri, R., Abdelly, C. & Gharsallli, M. (2007) Interactive effects of salinity and iron deficiency in *Medicago ciliaris*. *Comptes Rendus Biologies*, **330**(11), 779–788. Available from: <https://doi.org/10.1016/j.crvi.2007.08.007>
- Rahikainen, M., Pascual, J., Alegre, S., Durian, G. & Kangasjärvi, S. (2016) PP2A phosphatase as a regulator of ROS signaling in plants. *Antioxidants*, **5**(1), 8. Available from: <https://doi.org/10.3390/antiox5010008>
- Rai, S., Singh, P.K., Mankotia, S., Swain, J. & Satbhai, S.B. (2021) Iron homeostasis in plants and its crosstalk with copper, zinc, and manganese. *Plant Stress*, **1**, 100008. Available from: <https://doi.org/10.1016/j.plstres.2021.100008>
- Reddy, V.R.P., Das, S., Dikshit, H.K., Mishra, G.P., Aski, M., Meena, S.K. *et al.* (2020) Genome-wide association analysis for phosphorus use efficiency traits in mungbean (*Vigna radiata* L. Wilczek) using genotyping by sequencing approach. *Frontiers in Plant Science*, **11**, 537766. Available from: <https://doi.org/10.3389/fpls.2020.537766>
- Robert, F. & Pelletier, J. (2018) Exploring the impact of single-nucleotide polymorphisms on translation. *Frontiers in Genetics*, **9**, 507. Available from: <https://doi.org/10.3389/fgene.2018.00507>

- Rubio, F., Gassmann, W. & Schroeder, J.I. (1995) Sodium-driven potassium uptake by the plant potassium transporter HKT1 and mutations conferring salt tolerance. *Science*, **270**(5242), 1660–1663. Available from: <https://doi.org/10.1126/science.270.5242.1660>
- Rus, A., Baxter, I., Muthukumar, B., Gustin, J., Lahner, B., Yakubova, E. *et al.* (2006) Natural variants of At HKT1 enhance Na<sup>+</sup> accumulation in two wild populations of Arabidopsis. *PLoS Genetics*, **2**(12), e210. Available from: <https://doi.org/10.1371/journal.pgen.0020210>
- Saini, S., Kaur, N., Marothia, D., Singh, B., Singh, V., Gantet, P. *et al.* (2021) Morphological analysis, protein profiling and expression analysis of auxin homeostasis genes of roots of two contrasting cultivars of rice provide inputs on mechanisms involved in rice adaptation towards salinity stress. *Plants*, **10**(8), 1544. Available from: <https://doi.org/10.3390/plants10081544>
- Satbhai, S.B., Setzer, C., Freynschlag, F., Slovak, R., Kerdaffrec, E. & Busch, W. (2017) Natural allelic variation of FRO2 modulates Arabidopsis root growth under iron deficiency. *Nature Communications*, **8**(1), 1–10. Available from: <https://doi.org/10.1038/ncomms15603>
- Shabala, L., Cuin, T.A., Newman, I.A. & Shabala, S. (2005) Salinity-induced ion flux patterns from the excised roots of Arabidopsis sos mutants. *Planta*, **222**(6), 1041–1050. Available from: <https://doi.org/10.1007/s00425-005-0074-2>
- Shabala, S., Demidchik, V., Shabala, L., Cuin, T.A., Smith, S.J., Miller, A.J. *et al.* (2006) Extracellular Ca<sup>2+</sup> ameliorates NaCl-induced K<sup>+</sup> loss from Arabidopsis root and leaf cells by controlling plasma membrane K<sup>+</sup>-permeable channels. *Plant Physiology*, **141**(4), 1653–1665. Available from: <https://doi.org/10.1104/pp.106.082388>
- Shanmugam, V., Lo, J.C. & Yeh, K.C. (2013) Control of Zn uptake in Arabidopsis halleri: a balance between Zn and Fe. *Frontiers in Plant Science*, **4**, 281. Available from: <https://doi.org/10.3389/fpls.2013.00281>
- Shaul, O. (2002) Magnesium transport and function in plants: the tip of the iceberg. *Biomaterials*, **15**(3), 307–321. Available from: <https://doi.org/10.1023/A:1016091118585>
- Shi, D. & Sheng, Y. (2005) Effect of various salt-alkaline mixed stress conditions on sunflower seedlings and analysis of their stress factors. *Environmental and Experimental Botany*, **54**(1), 8–21. Available from: <https://doi.org/10.1016/j.envexpbot.2004.05.003>
- Shive, J.W. (1941) Significant roles of trace elements in the nutrition of plants. *Plant Physiology*, **16**(3), 435–445. Available from: <https://doi.org/10.1104/pp.16.3.435>
- Singh, A. (2021) Soil salinization management for sustainable development: a review. *Journal of Environmental Management*, **277**, 111383. Available from: <https://doi.org/10.1016/j.jenvman.2020.111383>
- Syed, N.H., Kalyana, M., Marquez, Y., Barta, A. & Brown, J.W. (2012) Alternative splicing in plants—coming of age. *Trends in Plant Science*, **17**(10), 616–623. Available from: <https://doi.org/10.1016/j.tplants.2012.06.001>
- Tan, S.T., Dai, C., Liu, H.T. & Xue, H.W. (2013) Arabidopsis casein kinase1 proteins CK1.3 and CK1.4 phosphorylate cryptochrome2 to regulate blue light signaling. *The Plant Cell*, **25**(7), 2618–2632. Available from: <https://doi.org/10.1105/tpc.113.114322>
- Terés, J. (2017) Characterization of natural populations of *A. thaliana* differing in tolerance to carbonate soil. Doctoral dissertation, Ph. D. Thesis Universitat Autònoma de Barcelona. <https://ddd.uab.cat/record/187700>
- Teschner, J., Lachmann, N., Schulze, J., Geisler, M., Selbach, K., Santamaria-Araujo, J. *et al.* (2010) A novel role for Arabidopsis mitochondrial ABC transporter ATM3 in molybdenum cofactor biosynthesis. *The Plant Cell*, **22**(2), 468–480. Available from: <https://doi.org/10.1105/tpc.109.068478>
- Tsydendambaev, V.D., Ivanova, T.V., Khalilova, L.A., Kurkova, E.B., Myasov, N.A. & Balnokin, Y.V. (2013) Fatty acid composition of lipids in vegetative organs of the halophyte *Suaeda altissima* under different levels of salinity. *Russian Journal of Plant Physiology*, **60**(5), 661–671. Available from: <https://doi.org/10.1134/S1021443713050142>
- Tuyen, D.D., Lal, S.K. & Xu, D.H. (2010) Identification of a major QTL allele from wild soybean (*Glycine soja* Sieb. & Zucc.) for increasing alkaline salt tolerance in soybean. *Theoretical and Applied Genetics*, **121**(2), 229–236. Available from: <https://doi.org/10.1007/s00122-010-1304-y>
- Uffemann, E., Huang, Q.Q., Munung, N.S., De Vries, J., Okada, Y., Martin, A.R. *et al.* (2021) Genome-wide association studies. *Nature Reviews Methods Primers*, **1**(1), 1–21. Available from: <https://doi.org/10.1038/s43586-021-00056-9>
- Ursache, R., Miyashima, S., Chen, Q., Vátén, A., Nakajima, K., Carlsbecker, A. *et al.* (2014) Tryptophan-dependent auxin biosynthesis is required for HD-ZIP III-mediated xylem patterning. *Development*, **141**(6), 1250–1259. Available from: <https://doi.org/10.1242/dev.103473>
- Vert, G., Briat, J.F. & Curie, C. (2001) Arabidopsis IRT2 gene encodes a root-periphery iron transporter. *The Plant Journal*, **26**(2), 181–189. Available from: <https://doi.org/10.1046/j.1365-3113x.2001.01018.x>
- Vigani, G. & Briat, J.F. (2016) Impairment of respiratory chain under nutrient deficiency in plants: does it play a role in the regulation of iron and sulfur responsive genes? *Frontiers in Plant Science*, **6**, 1185. Available from: <https://doi.org/10.3389/fpls.2015.01185>
- Volkmar, K.M., Hu, Y. & Steppuhn, H. (1998) Physiological responses of plants to salinity: a review. *Canadian Journal of Plant Science*, **78**(1), 19–27. Available from: <https://doi.org/10.4141/P97-020>
- Voogt, W. (1988) The growth of beefsteak tomato as affected by K/Ca ratios in the nutrient solution. *Acta Horticulturae*, **222**, 155–166. Available from: <https://doi.org/10.17660/ActaHortic.1988.222.18>
- Wang, T., Yu, Q., Chen, J., Deng, B., Qian, L. & Le, Y. (2010) PP2A mediated AMPK inhibition promotes HSP70 expression in heat shock response. *PLoS One*, **5**(10), e13096. Available from: <https://doi.org/10.1371/journal.pone.0013096>
- Wang, X., Tucker, N.R., Rizki, G., Miller, R., Krijger, P.H.L., de Wit, E. *et al.* (2016) Discovery and validation of sub-threshold genome-wide association study loci using epigenomic signatures. *eLife*, **5**, e10557. Available from: <https://doi.org/10.7554/eLife.10557>
- Warraich, A.S., Krishnamurthy, S.L., Sooch, B.S., Vinaykumar, N.M., Dushyanthkumar, B.M., Bose, J. *et al.* (2020) Rice GWAS reveals key genomic regions essential for salinity tolerance at reproductive stage. *Acta Physiologicae Plantarum*, **42**(8), 1–15. Available from: <https://doi.org/10.1007/s11738-020-03123-y>
- Weigel, D. (2012) Natural variation in Arabidopsis: from molecular genetics to ecological genomics. *Plant Physiology*, **158**(1), 2–22. Available from: <https://doi.org/10.1104/pp.111.189845>
- Xu, J., Xu, W., Chen, X., Zhu, H., Fu, X. & Yu, F. (2022) Genome-wide association analysis reveals the genetic bases of iron-deficiency stress tolerance in maize. *Frontiers in Plant Science*, **13**, 878809. Available from: <https://doi.org/10.3389/fpls.2022.878809>
- Yasir, M., He, S., Sun, G., Geng, X., Pan, Z., Gong, W. *et al.* (2019) A genome-wide association study revealed key SNPs/genes associated with salinity stress tolerance in upland cotton. *Genes*, **10**(10), 829. Available from: <https://doi.org/10.3390/genes10100829>
- Ye, X., Wang, H., Cao, X., Jin, X., Cui, F., Bu, Y. *et al.* (2019) Transcriptome profiling of *Puccinellia tenuiflora* during seed germination under a long-term saline-alkali stress. *BMC Genomics*, **20**, 589. Available from: <https://doi.org/10.1186/s12864-019-5860-5>
- Yousfi, S., Mahmoudi, H., Abdely, C. & Gharsalli, M. (2007) Effect of salt on physiological responses of barley to iron deficiency. *Plant Physiology and Biochemistry*, **45**(5), 309–314. Available from: <https://doi.org/10.1016/j.plaphy.2007.03.013>
- Yuan, Y., Wu, H., Wang, N., Li, J., Zhao, W., Du, J. *et al.* (2008) FIT interacts with AtbHLH38 and AtbHLH39 in regulating iron uptake gene expression for iron homeostasis in Arabidopsis. *Cell Research*, **18**(3), 385–397. Available from: <https://doi.org/10.1038/cr.2008.26>
- Zeng, A., Chen, P., Korth, K., Hancock, F., Pereira, A., Brye, K. *et al.* (2017) Genome-wide association study (GWAS) of salt tolerance in worldwide soybean germplasm lines. *Molecular Breeding*, **37**(3), 1–14. Available from: <https://doi.org/10.1007/s11032-017-0634-8>
- Zhang, R., Xu, C., Bao, Z., Xiao, R., Chen, X., Xiao, W. *et al.* (2021) Auxin alters sodium ion accumulation and nutrient accumulation by playing protective role in salinity challenged strawberry. *Plant Physiology and Biochemistry*, **164**, 1–9. Available from: <https://doi.org/10.1016/j.plaphy.2021.04.008>
- Zhang, W., Liao, X., Cui, Y., Ma, W., Zhang, X., Du, H. *et al.* (2019) A cation diffusion facilitator, GmCDF1, negatively regulates salt tolerance in soybean. *PLoS Genetics*, **15**(1), e1007798. Available from: <https://doi.org/10.1371/journal.pgen.1007798>
- Zhang, W.J., Niu, Y., Bu, S.H., Li, M., Feng, J.Y., Zhang, J. *et al.* (2014) Epistatic association mapping for alkaline and salinity tolerance traits in the soybean germination stage. *PLoS One*, **9**(1), e84750. Available from: <https://doi.org/10.1371/journal.pone.0084750>
- Zhang, X., Adamowski, M., Marhava, P., Tan, S., Zhang, Y., Rodriguez, L. *et al.* (2020) Arabidopsis flippases cooperate with ARF GTPase exchange factors to regulate the trafficking and polarity of PIN auxin transporters.

- The Plant Cell*, **32**(5), 1644–1664. Available from: <https://doi.org/10.1105/tpc.19.00869>
- Zhang, J.T. & Mu, C.S.** (2009) Effects of saline and alkaline stresses on the germination, growth, photosynthesis, ionic balance, and anti-oxidant system in an alkali-tolerant leguminous forage *Lathyrus quinquenervius*. *Soil Science & Plant Nutrition*, **55**(5), 685–697. Available from: <https://doi.org/10.1111/j.1747-0765.2009.00411.x>
- Zhao, Y., Wang, G., Zhao, M., Wang, M., Xue, Z., Liu, B. et al.** (2021) Seed limitation and saline-alkaline stress restrict wetland restoration potential in the Songnen plain, northeastern China. *Ecological Indicators*, **129**, 107998. Available from: <https://doi.org/10.1016/j.ecolind.2021.107998>
- Zhou, C., Zhu, L., Xie, Y., Li, F., Xiao, X., Ma, Z. et al.** (2017) *Bacillus licheniformis* SA03 confers increased saline-alkaline tolerance in chrysanthemum plants by induction of abscisic acid accumulation. *Frontiers in Plant Science*, **8**, 1143. Available from: <https://doi.org/10.3389/fpls.2017.011143>
- Zhou, X. & Stephens, M.** (2012) Genome-wide efficient mixed-model analysis for association studies. *Nature Genetics*, **44**(7), 821–824. Available from: <https://doi.org/10.1038/ng.2310>